

Appendix to report:

SBJ-33-C5-OON-22-RE-014-B

K12 - SHIP IMPACT, PONTOONS AND COLUMNS

Appendix title:

APPENDIX C - SENSITIVITY OF SHIP IMPACT RESPONSE

Contract no: 18/91094
Project number: 5187772/12777
Document number: SBJ-33-C5-OON-22-RE-014-B App. C

Date: 15.08.2019
Revision: 0
Number of pages: 50

Prepared by: Thanh Ngan Nguyen
Controlled by: Eivind Bjørhei
Approved by: Kolbjørn Høyland

CONCEPT DEVELOPMENT FLOATING BRIDGE E39 BJØRNAFJORDEN



Table of Content

1	SENSITIVITY OF SUPERDUPLEX STEEL	3
2	SENSITIVITY OF MATERIAL PARAMETERS – CONTAINER BOW	6
3	SENSITIVITY OF MATERIAL PARAMETERS – ICE- STRENGTHENED BOW	15
4	SENSITIVITY OF MATERIAL DAMAGE MODELS	21
5	SENSITIVITY OF MESH SIZE AND ELEMENT TYPE	28
6	SENSITIVITY OF IMPACT HEIGHT AND VELOCITY	37
7	CONTROL OF ENERGY BALANCE.....	44
8	REFERENCES	50

1 SENSITIVITY OF SUPERDUPLEX STEEL

This section shows results when utilizing superduplex steel material in the splash zone. The sensitivity of superduplex steel is investigated for the container bow.

The splash zone for the pontoon outer walls is from 1.3 m below to 1.7 m above the water level. The material parameters and curve of the superduplex steel are given in [1] Table 4-1 and Figure 4-11. The material utilized for the pontoon outside the splash zone and for the ship bow is equal to the "mean-low" material.

Figure 1-1 shows the force-displacement curves for the models with superduplex steel compared with the reference curves. It is seen that the initial impact is almost identical.

ID-no.	Max. contact force [MN] 0-4 m	Mean contact force [MN] 0-4 m
55	34	27
52	27	21
50	34	26
51	33	23

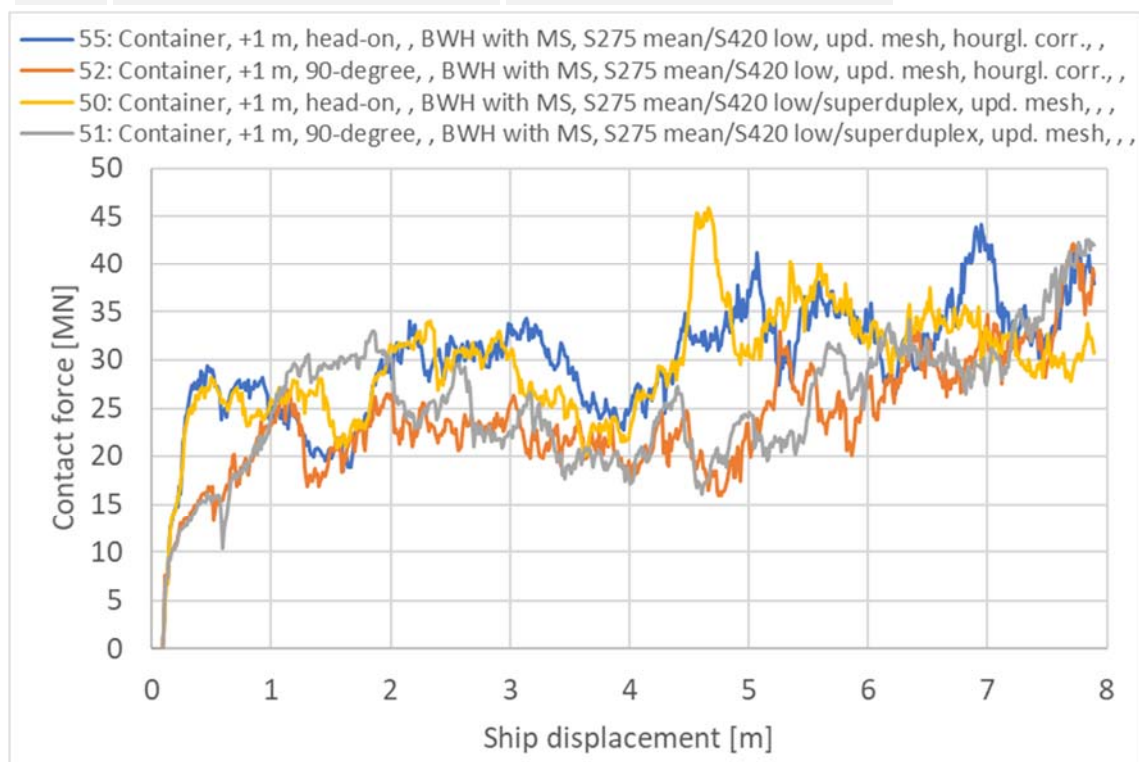


> Figure 1-1 Contact force [MN] impact bow-pontoon, sensitivity of superduplex steel

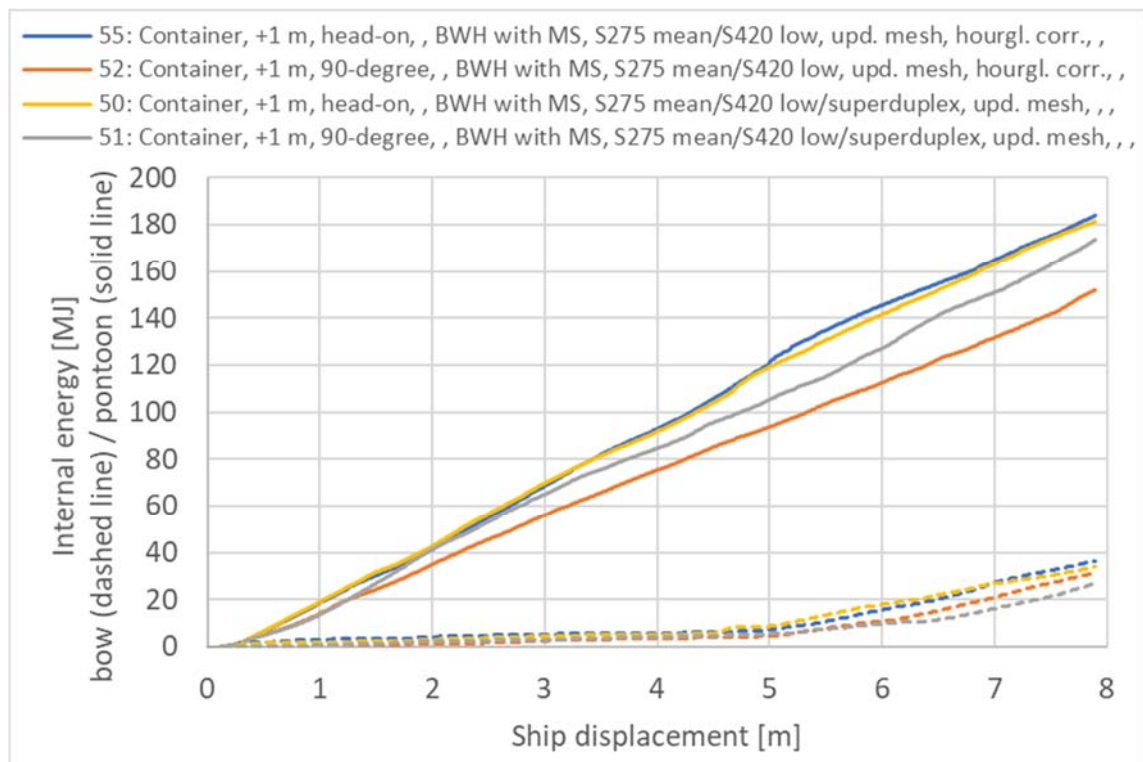
Figure 1-2 shows the internal energy dissipated in the bow with dashed line and the pontoon with solid line. It is seen that the internal energy is identical for the head-on impact between the superduplex steel material and the standard steel material. The 90-degree impact results in a bit higher energy with superduplex steel.

Figure 1-3 shows the frictional dissipation and artificial energy in the models. The proportion of artificial to internal energy is 9-11 % for the displayed models. The frictional dissipation is a bit higher for the head-on impact with superduplex steel, but lower for the 90-degree impact. The artificial energy reflects the internal energy in the models.

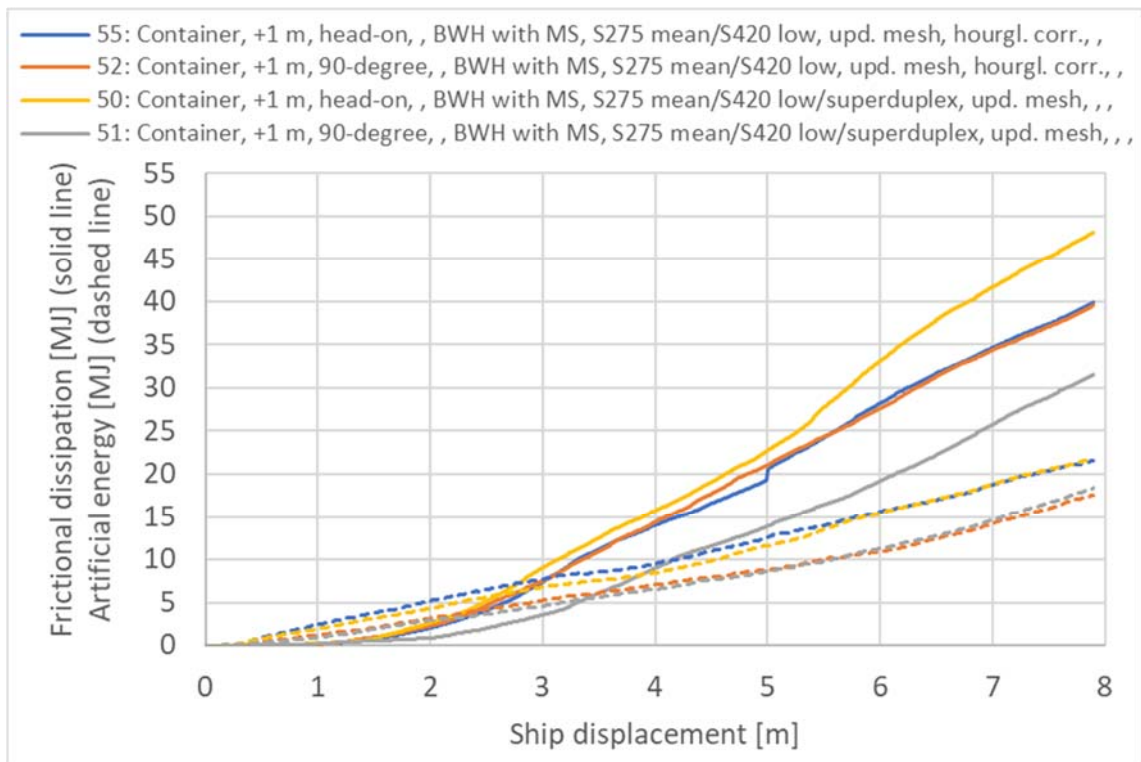
The discontinuity in the frictional dissipation for the head-on impact with standard steel material is due to contact disturbances in the model. These disturbances are non-existing when utilizing the superduplex steel material.

Figure 1-4 shows that the proportion of internal energy dissipated in the pontoon is high and that the superduplex steel does not affect the results much.

The models with superduplex steel affect the impact results to both lower and higher force and energy level, but the differences are not prominent.



> Figure 1-2 Internal energy [MJ] impact bow-pontoon, sensitivity of superduplex steel



> Figure 1-3 Frictional dissipation and artificial energy [MJ] impact bow-pontoon, sensitivity of superduplex steel

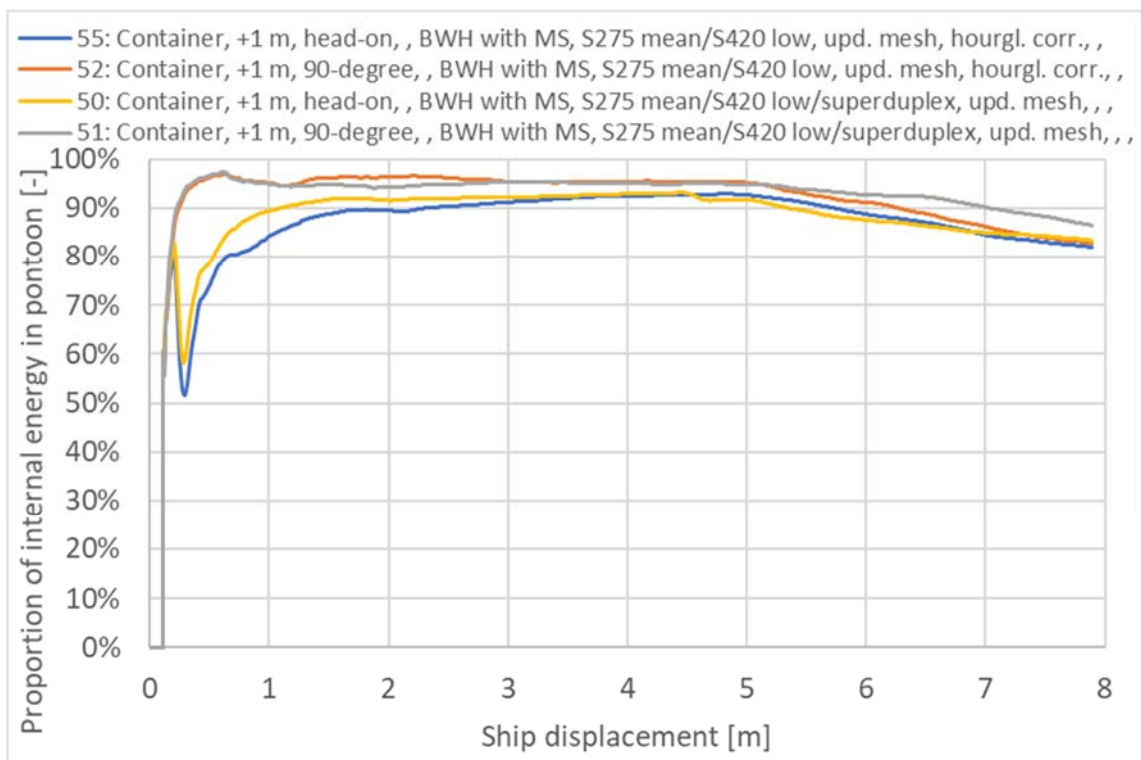


> Figure 1-4 Proportion of internal energy in pontoon [-] impact bow-pontoon, sensitivity of superduplex steel

2 SENSITIVITY OF MATERIAL PARAMETERS – CONTAINER BOW

This section investigates the sensitivity of material parameters for impact with the container bow. The material damage model used is the BWH model with mesh scaling. The different material parameters chosen are shown in Table 2-1. The resulting material curves are shown in Figure 2-1 to Figure 2-3. S275 is utilized for the ship bows, S355 for the pontoon stiffeners and S420 for the pontoon plates.

> *Table 2-1 Material parameters for sensitivity analyses*

Name	Steel quality	Yield stress ¹	$\epsilon_{\text{plateau}}$	K	n
Low ²	S275	276.5 MPa	0.017	620 MPa	0.166
	S355	357 MPa	0.015	740 MPa	0.166
	S420	422.5 MPa	0.012	738 MPa	0.140
Mean ³	S275	331.8 MPa	0.017	740 MPa	0.166
	S355	428.4 MPa	0.015	900 MPa	0.166
	S420	485.9 MPa	0.011928571	738 MPa	0.140
Mean-high ⁴	S275	331.8 MPa	0.017	740 MPa	0.166
	S355	428.4 MPa	0.015	1002 MPa	0.166
	S420	485.9 MPa	0.011928571	1030 MPa	0.140
Mean-low ⁵	S275	331.8 MPa	0.017	764 MPa	0.185
	S355	357 MPa	0.015	796 MPa	0.178
	S420	422.5 MPa	0.012	827 MPa	0.155

¹ For thicknesses 16 mm and below

² Equal to material in section 4.2 [1], bullet 1

³ Parameters according to DNVGL-RP-C208 [4] section 7.8

⁴ Yield stress, $\epsilon_{\text{plateau}}$ and n according to DNVGL-RP-C208 [4] section 7.8, K according to section 4.2 [1], bullet 2.c and 2.d

⁵ Equal to material in section 4.2 [1], bullet 1

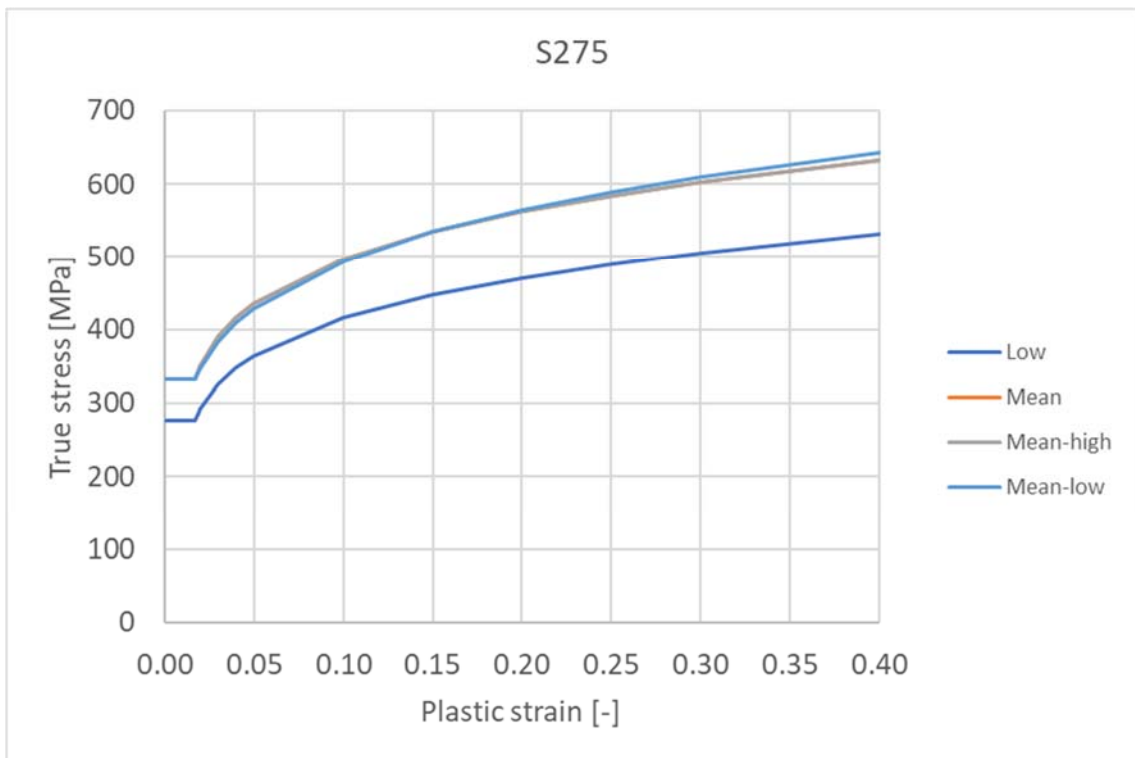


> Figure 2-1 True stress-strain curves of the S275 steel materials for sensitivity analyses ("mean" and "mean-high" are equal)

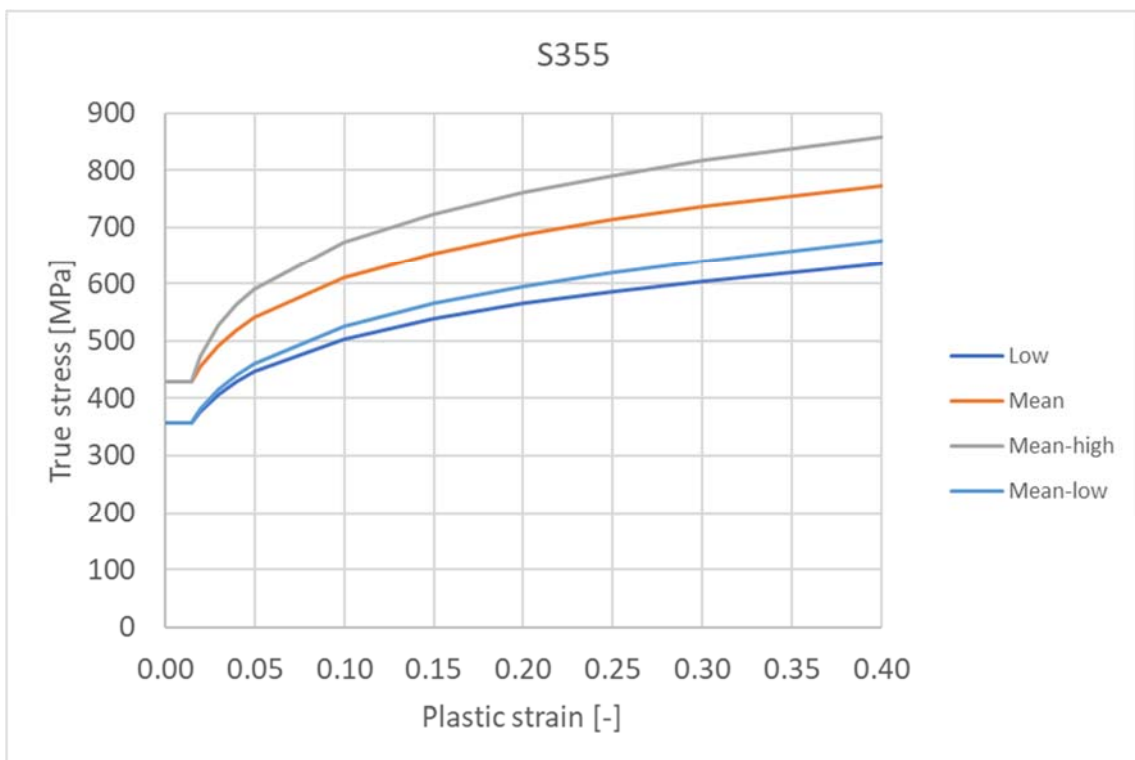


> Figure 2-2 True stress-strain curves of the S355 steel materials for sensitivity analyses

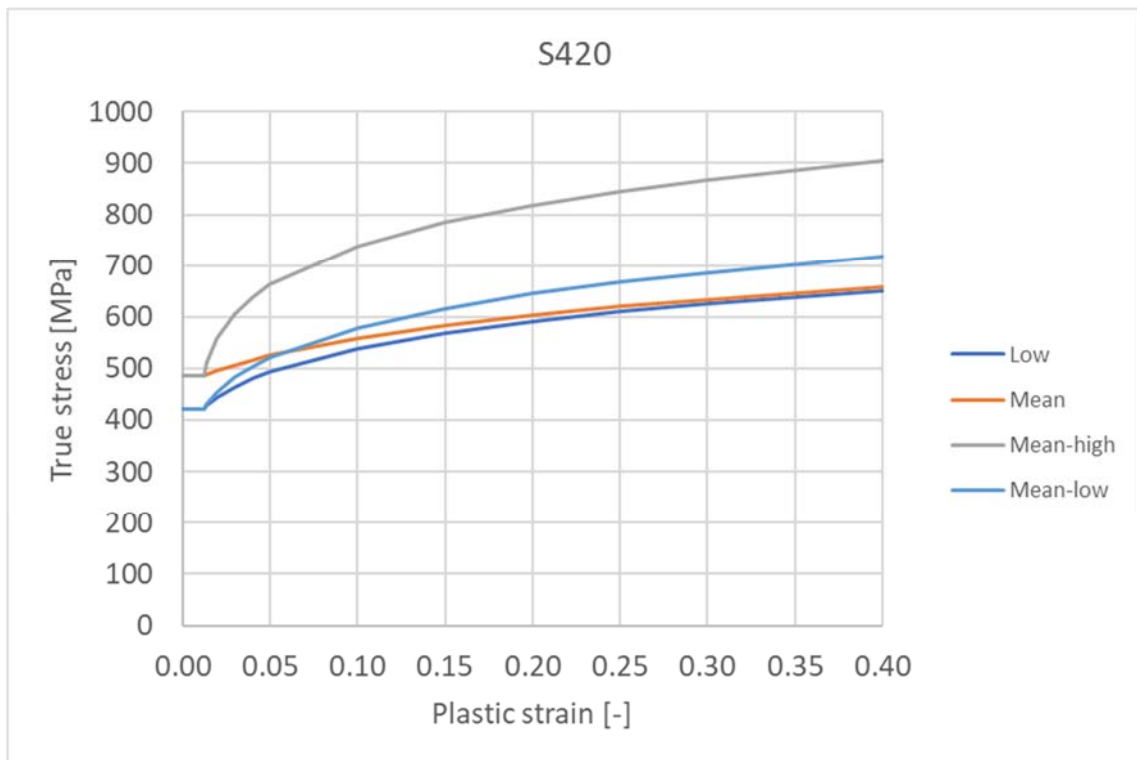


> Figure 2-3 True stress-strain curves of the S420 steel materials for sensitivity analyses

Figure 2-4 and Figure 2-5 show the force-displacement curves for the sensitivity check of material parameters with the container bow. The choice of material parameters affects the collision response. The initial impact is almost identical with “low”, “mean” and “mean-low” material, while the “mean-high” material results in higher impact force. The “mean” material gave deviant results for the head-on impact, and thus considered not to be the best material to choose for the local ship impact analyses.

The “low” material is a set of parameters intended for design calculations. The design parameters may result in too low capacity for structures when the goal is to evaluate the impact forces. On the other hand, the “mean-high” material is considered too conservative. Since the bridge is designed utilizing low material properties, the “mean-low” material seems more holistic to utilize for the pontoons when evaluating the ship impact response. The “mean-low” material parameters are also close to the material parameters chosen for the work performed at NTNU [2] and by the suspension bridge group [3] in the previous phases of the Bjørnafjorden project.

ID-no.	Max. contact force [MN] 0-4 m	Mean contact force [MN] 0-4 m
17	30	14
29	40	30
56	33	24
55	34	27

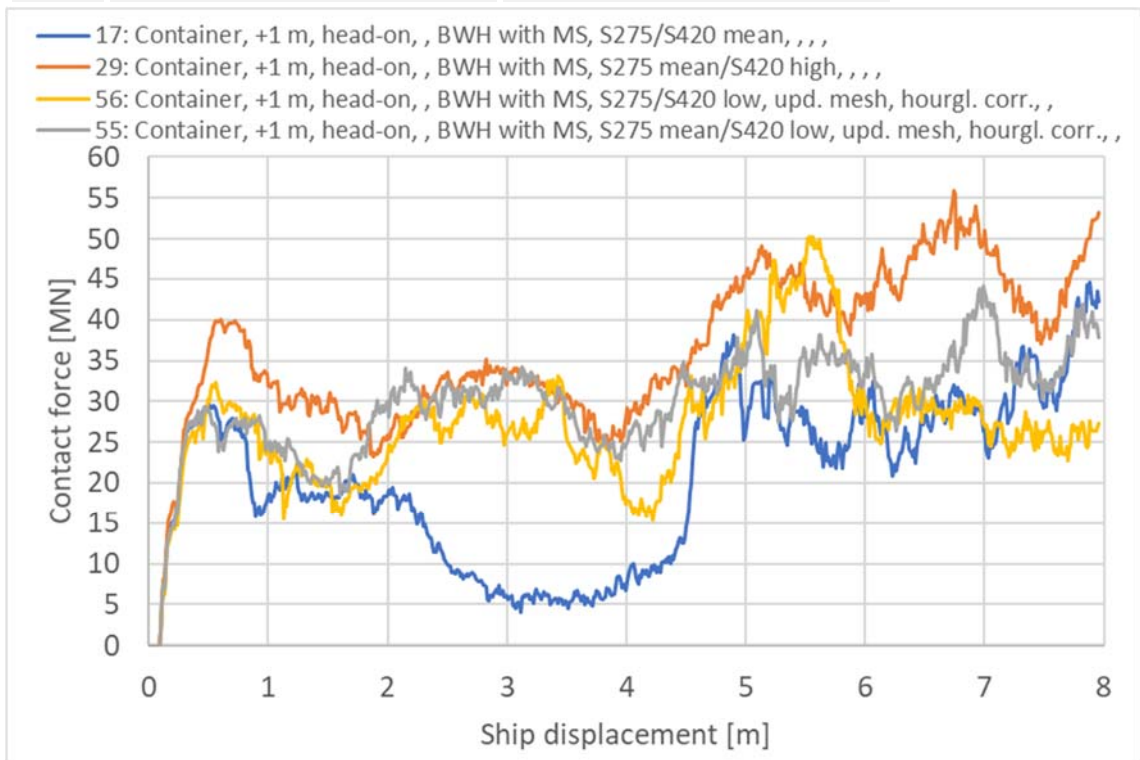


> Figure 2-4 Contact force [MN] impact container bow-pontoon head-on, sensitivity of material parameters

ID-no.	Max. contact force [MN] 0-4 m	Mean contact force [MN] 0-4 m
21	24	17
35	40	28
32	25	17
52	27	21

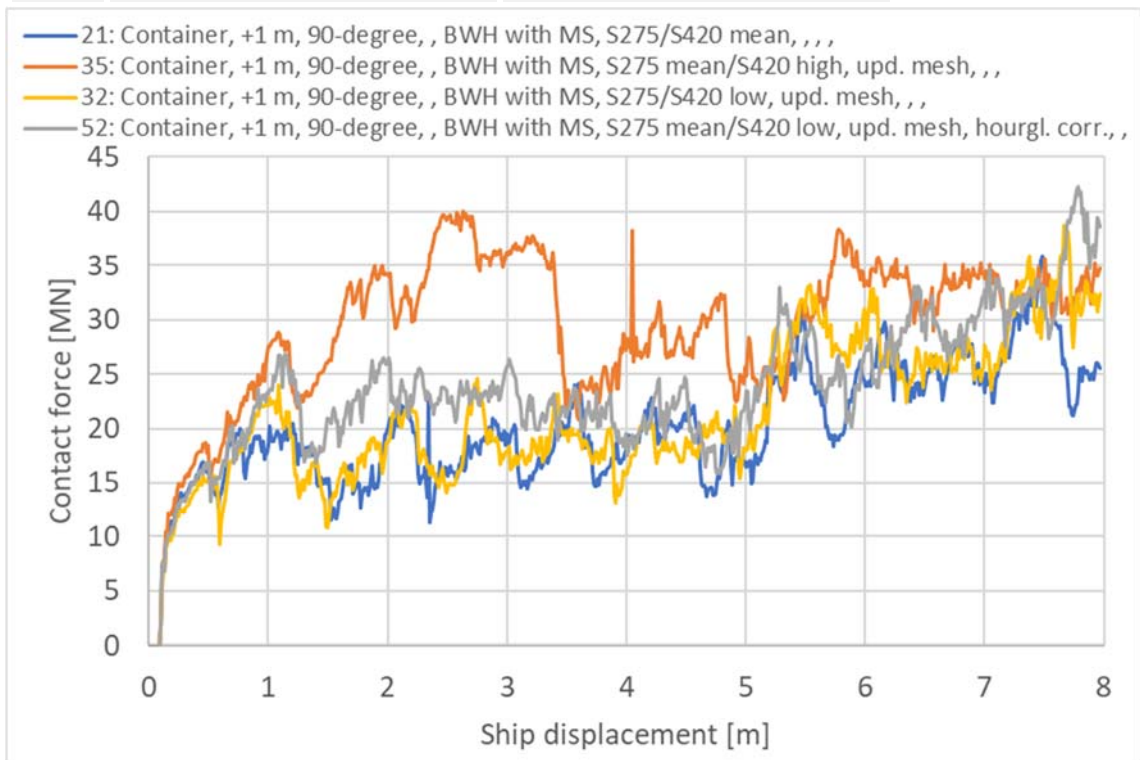
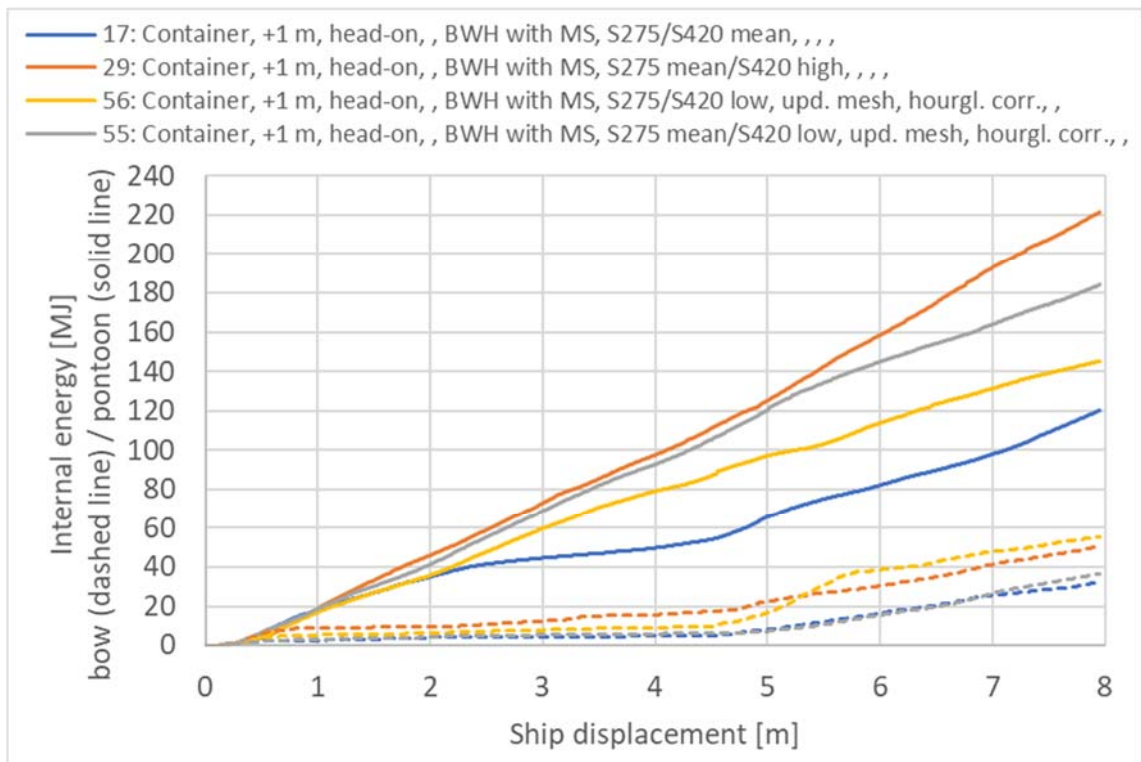


> Figure 2-5 Contact force [MN] impact container bow-pontoon 90-degree, sensitivity of material parameters

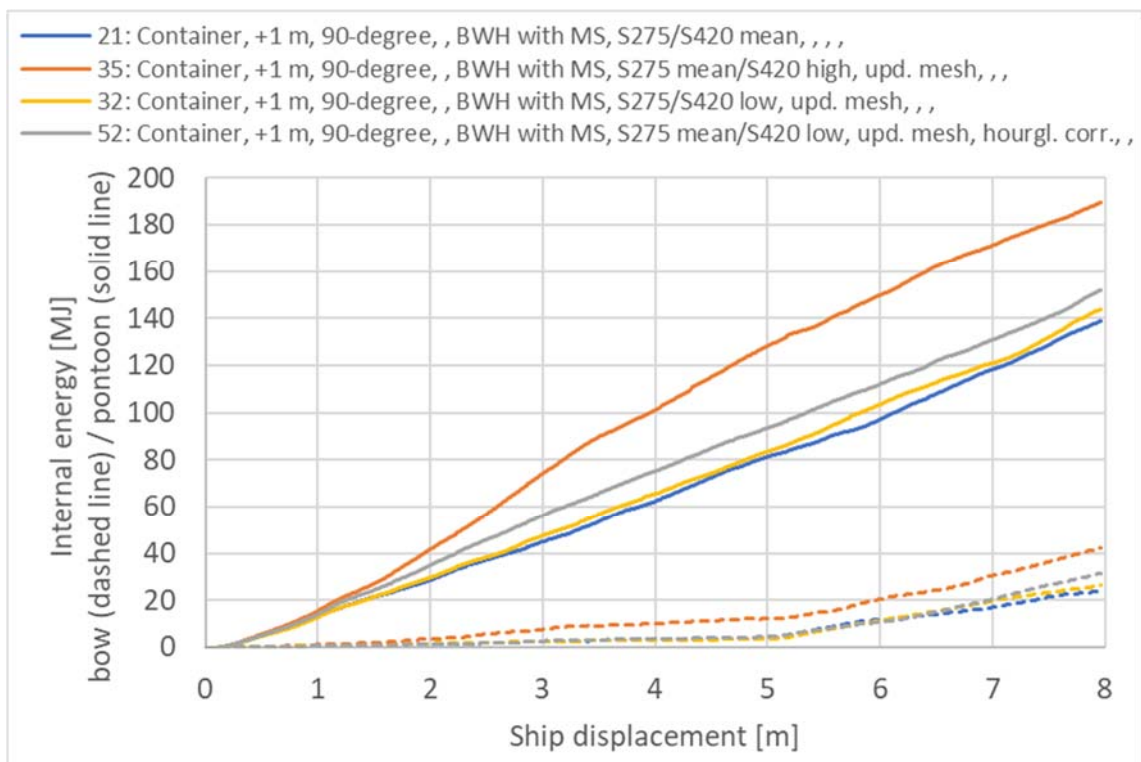
Figure 2-6 and Figure 2-7 show the internal energy dissipated in the bow with dashed line and the pontoon with solid line. The internal energy is highest for response with the “mean-high” material. The ship bow is less sensitive for the choice of material parameters than the pontoon.

Figure 2-8 and Figure 2-9 show the frictional dissipation and artificial energy in the models. The proportion of artificial to internal energy is 9-12 % for the displayed models.

Figure 2-10 and Figure 2-11 show the proportion of internal energy dissipated in the pontoon. The dissipated energy is high, with the “mean-high” material giving a bit lower energy dissipation in the pontoon in the early stage of the head-on impact with the container bow.



> Figure 2-6 Internal energy [MJ] impact container bow-pontoon head-on, sensitivity of material parameters



> Figure 2-7 Internal energy [MJ] impact container bow-pontoon 90-degree, sensitivity of material parameters

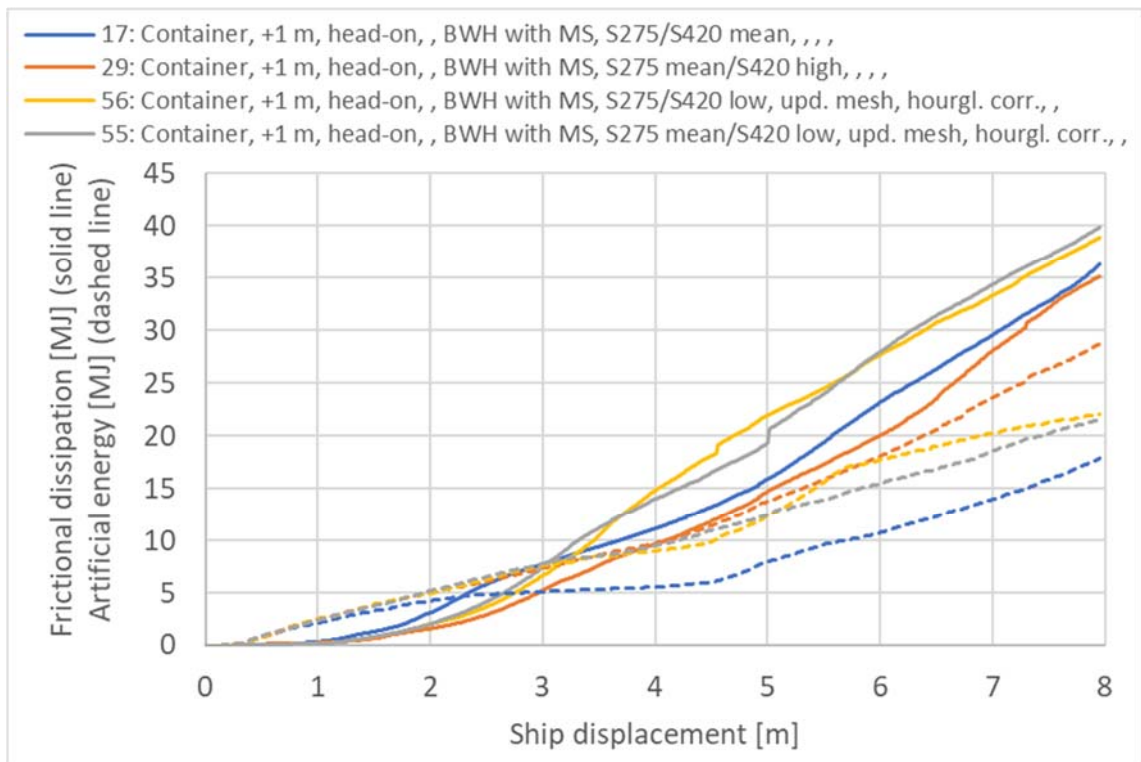


> Figure 2-8 Frictional dissipation and artificial energy [MJ] impact container bow-pontoon head-on, sensitivity of material parameters

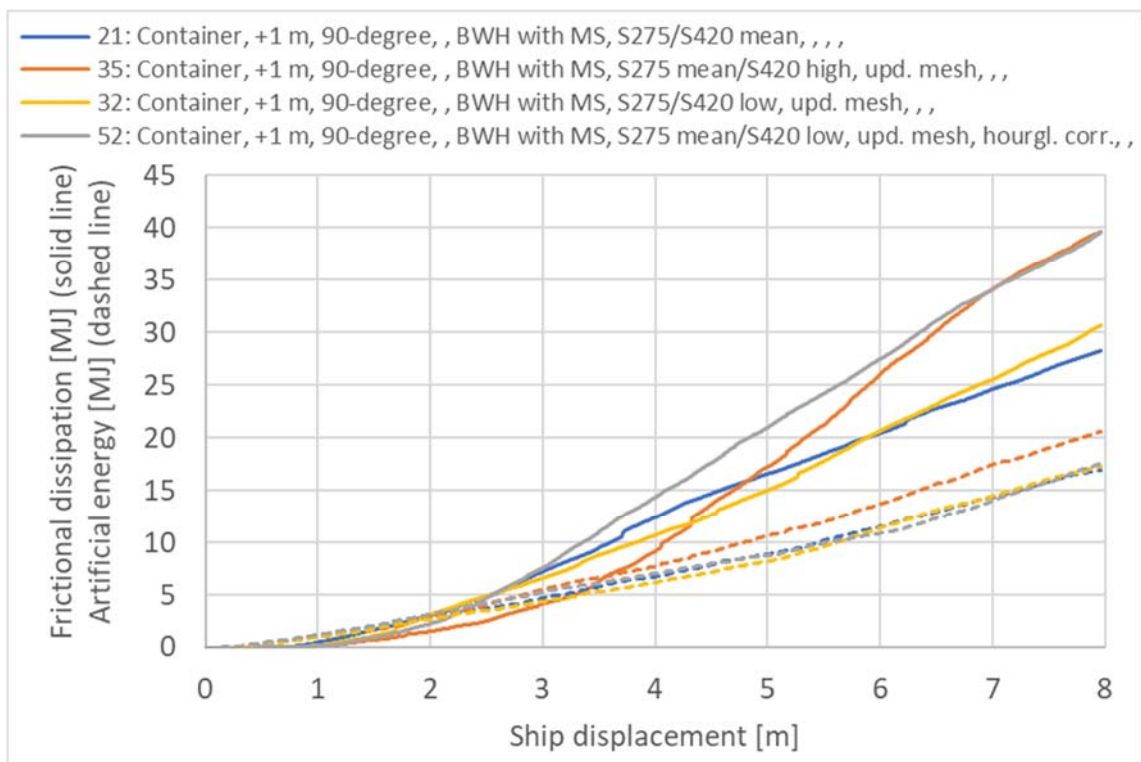


> Figure 2-9 Frictional dissipation and artificial energy [MJ] impact container bow-pontoon 90-degree, sensitivity of material parameters

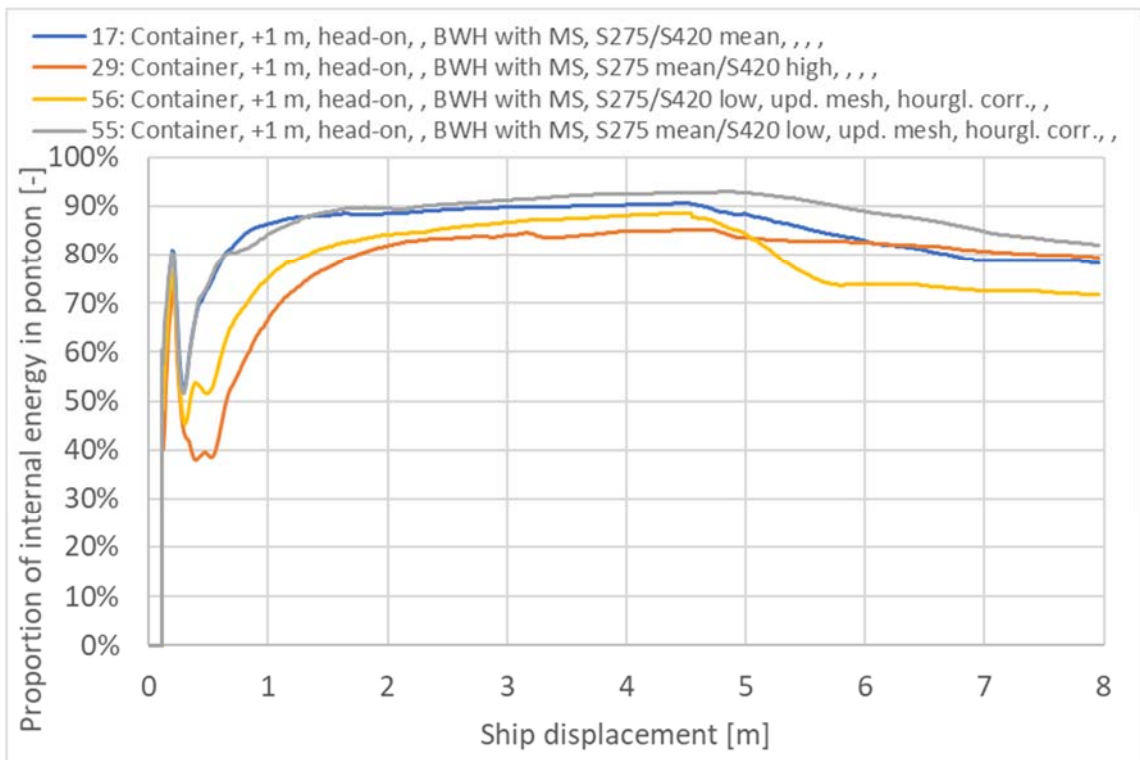


> Figure 2-10 Proportion of internal energy in pontoon [-] impact container bow-pontoon head-on, sensitivity of material parameters

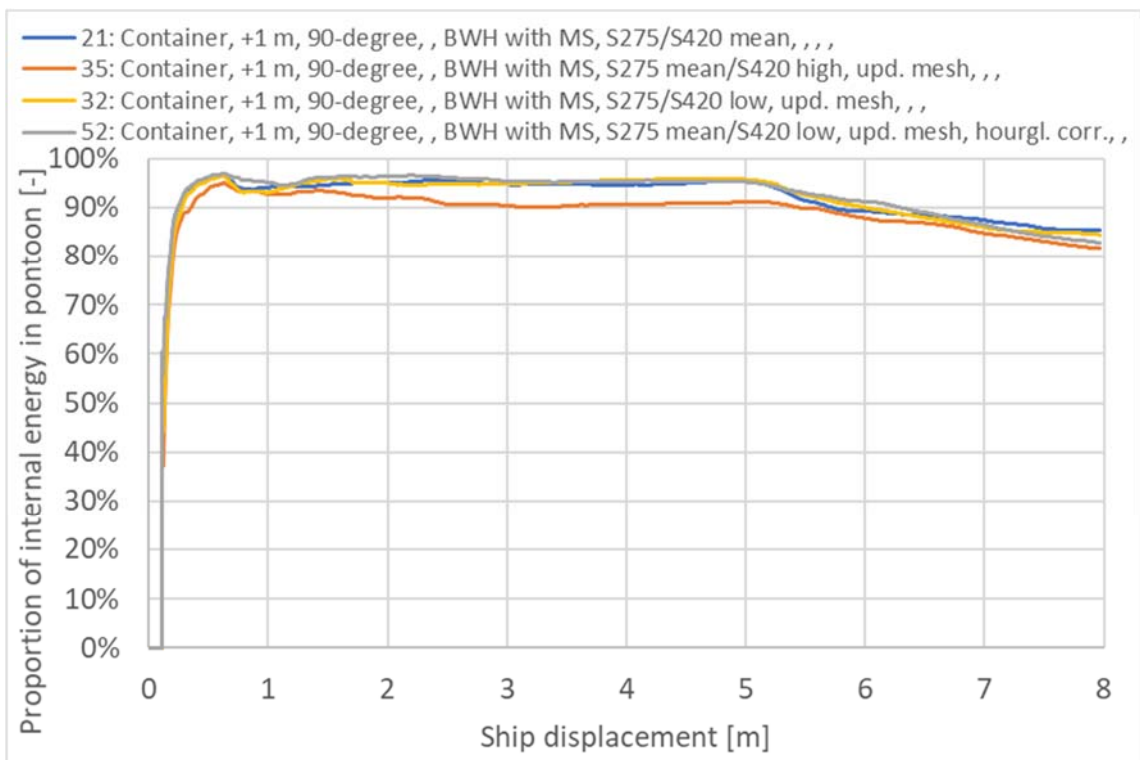


> Figure 2-11 Proportion of internal energy in pontoon [-] impact container bow-pontoon 90-degree, sensitivity of material parameters

Figure 2-12 shows a graphical presentation of the sensitivity of the material parameters investigated for impact with the container bow. An equal value of the dissipated internal energy in the local simulations is chosen, 100 MJ. This is about 40 % of the energy to be dissipated in axis 3 (246 MJ). Then, the maximum contact force occurred from 0 m ship displacement to ship displacement corresponding 100 MJ for the respective simulation is evaluated. I.e. the maximum force from Figure 2-4 and Figure 2-5, defined by a cut-off at 100 MJ for the respective simulation.

It is seen that the "mean-high" set of material parameters gives the shortest ship displacement at 100 MJ and the highest maximum contact force. The simulation is sensitive to especially the "mean-high" set of material parameters. In addition, head-on impact with the "mean" material according to DNVGL-RP-C208 [4] gave deviant results.

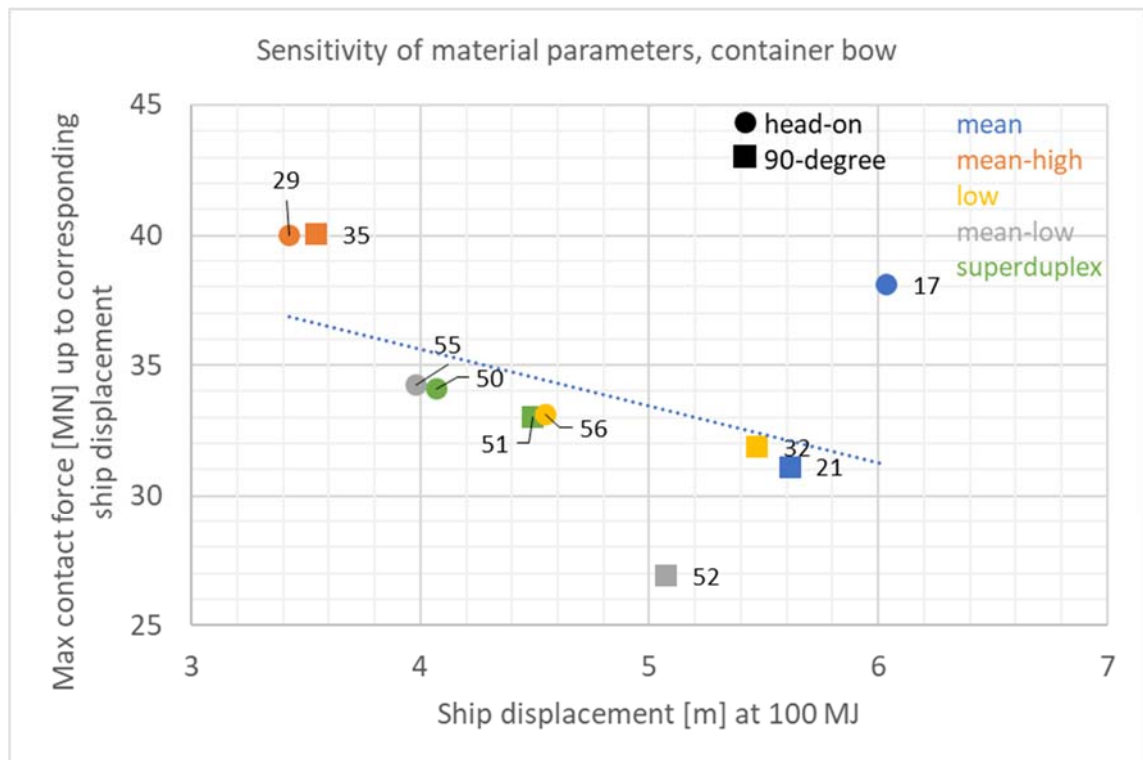


> Figure 2-12 Sensitivity of material parameters, impact container bow-pontoon

3 SENSITIVITY OF MATERIAL PARAMETERS – ICE-STRENGTHENED BOW

This section investigates the sensitivity of material parameters for impact with the ice-strengthened bow. The material damage model used is the BWH model with mesh scaling. The different material parameters chosen are described in section 2.

Figure 3-1 and Figure 3-2 show the force-displacement curves for the sensitivity check of material parameters with the ice-strengthened bow. The choice of material parameters affects the collision response. However, the initial impact is almost identical with “low”, “mean” and “mean-low” material, while the “mean-high” material results in higher impact force.

The “mean-low” material is chosen for the base impact cases with reference to the discussion in section 2.

ID-no.	Max. contact force [MN] 0-4 m	Mean contact force [MN] 0-4 m
24	19	10
43	25	15
45	17	11
48	19	11

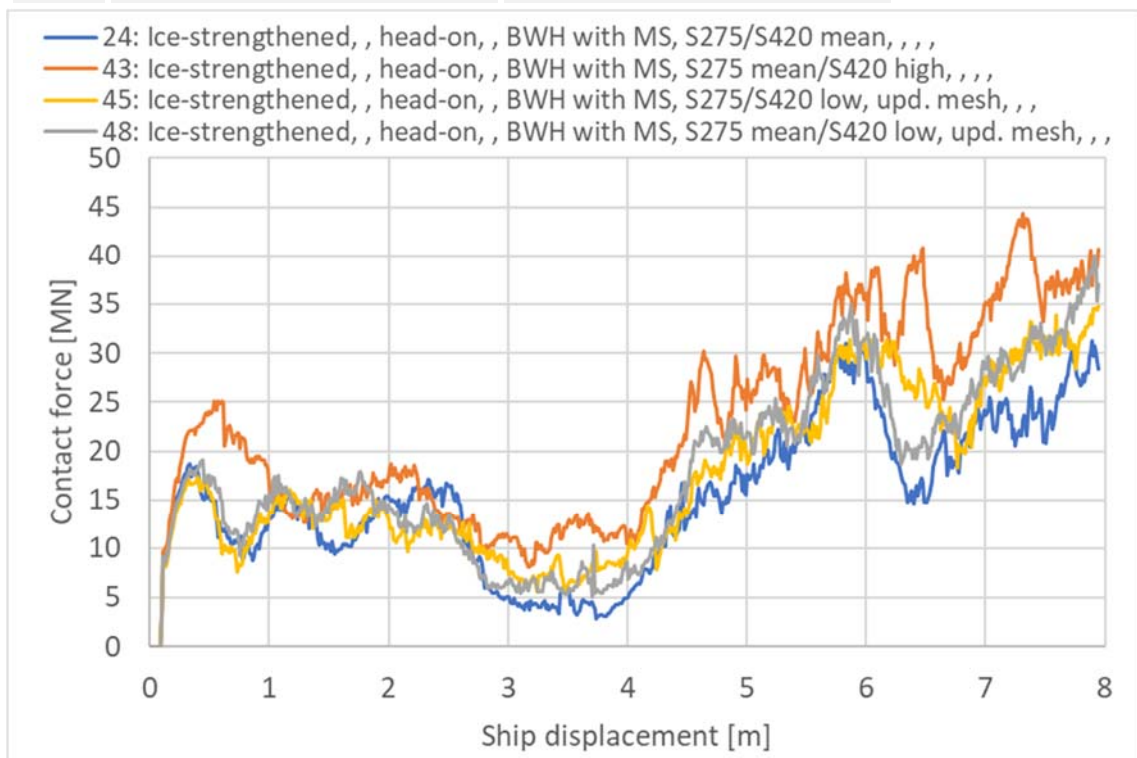


> Figure 3-1 Contact force [MN] impact ice-strengthened bow-pontoon head-on, sensitivity of material parameters

ID-no.	Max. contact force [MN] 0-4 m	Mean contact force [MN] 0-4 m
26	14	10
44	26	16
46	15	11
49	22	13

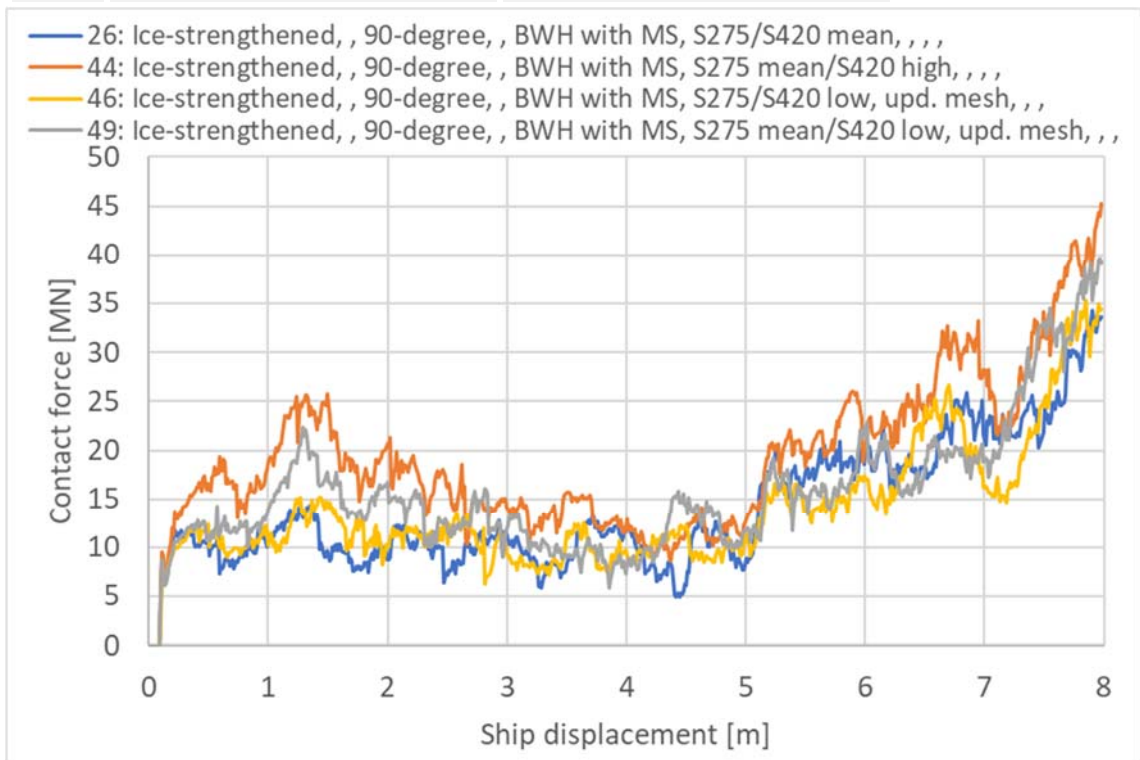
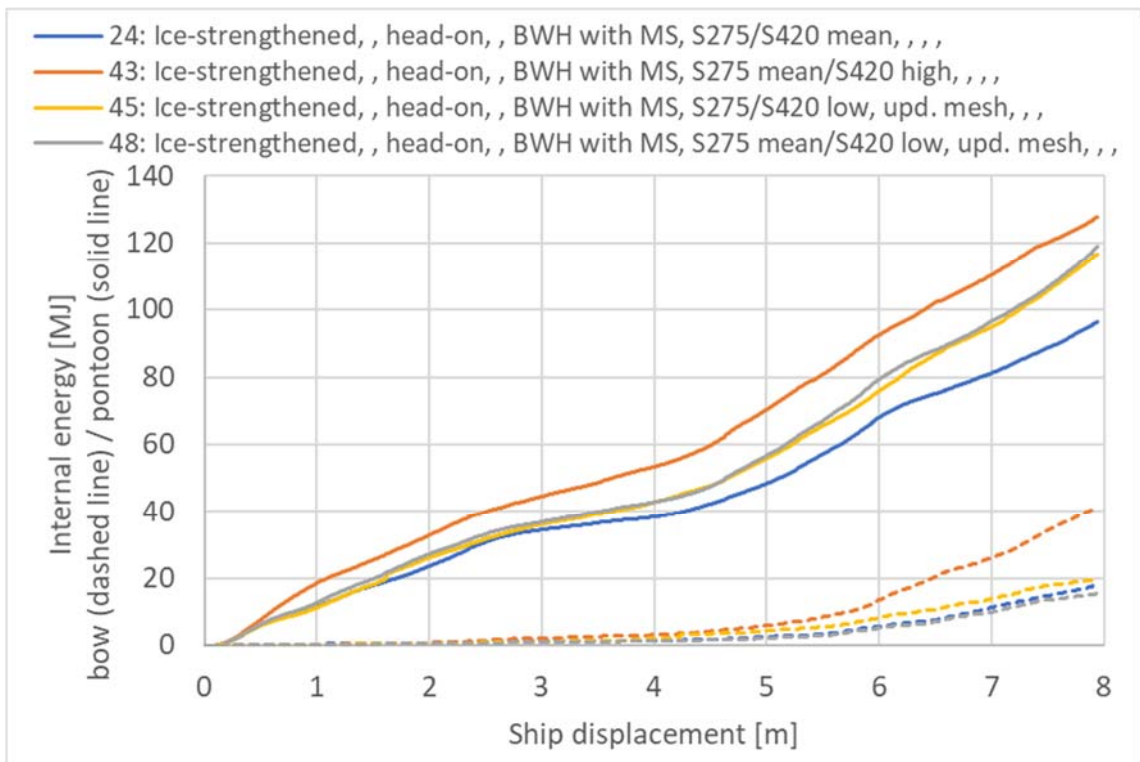


> Figure 3-2 Contact force [MN] impact ice-strengthened bow-pontoon 90-degree, sensitivity of material parameters

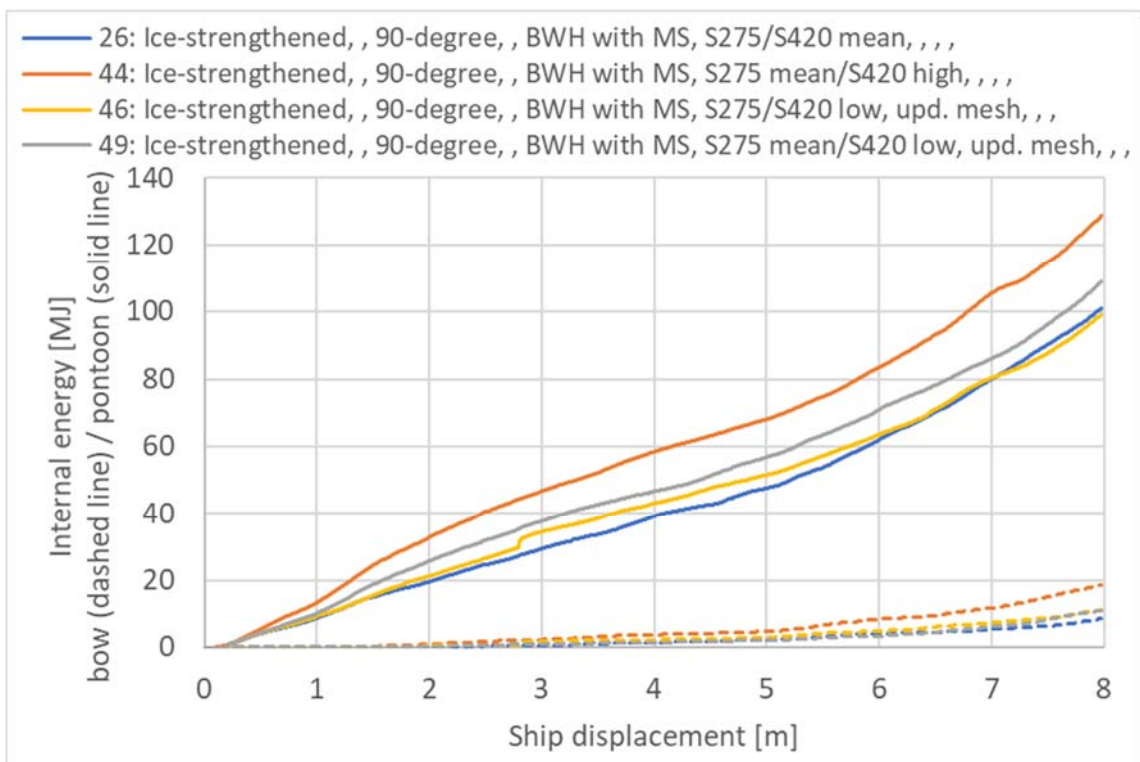
Figure 3-3 and Figure 3-4 show the internal energy dissipated in the bow with dashed line and the pontoon with solid line. The internal energy is highest for response with the “mean-high” material. The ship bow is less sensitive for the choice of material parameters than the pontoon.

Figure 3-5 and Figure 3-6 show the frictional dissipation and artificial energy in the models. The proportion of artificial to internal energy is 9-12 % for the displayed models.

Figure 3-7 and Figure 3-8 show the proportion of internal energy dissipated in the pontoon. The dissipated energy is high for all models, with the “mean-high” material giving slightly lower energy dissipation in the pontoon in the late stage of the head-on impact with the ice-strengthened bow.



> Figure 3-3 Internal energy [MJ] impact ice-strengthened bow-pontoon head-on, sensitivity of material parameters



> Figure 3-4 Internal energy [MJ] impact ice-strengthened bow-pontoon 90-degree, sensitivity of material parameters

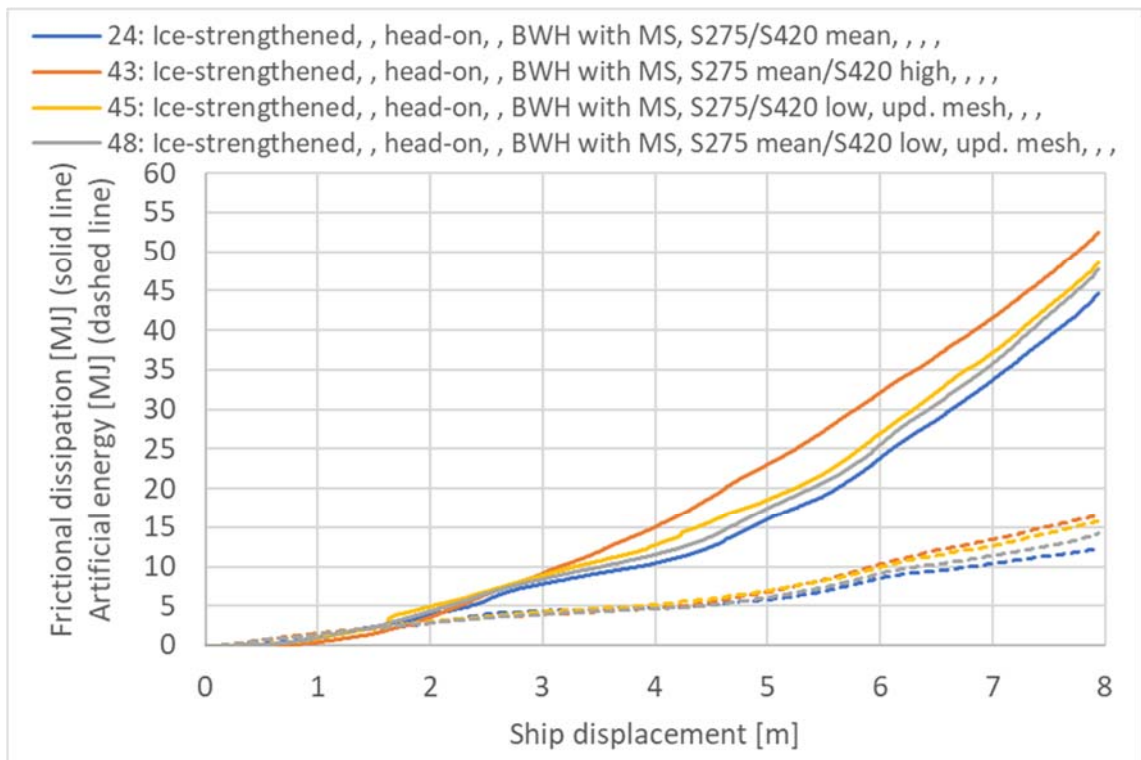


> Figure 3-5 Frictional dissipation and artificial energy [MJ] impact ice-strengthened bow-pontoon head-on, sensitivity of material parameters

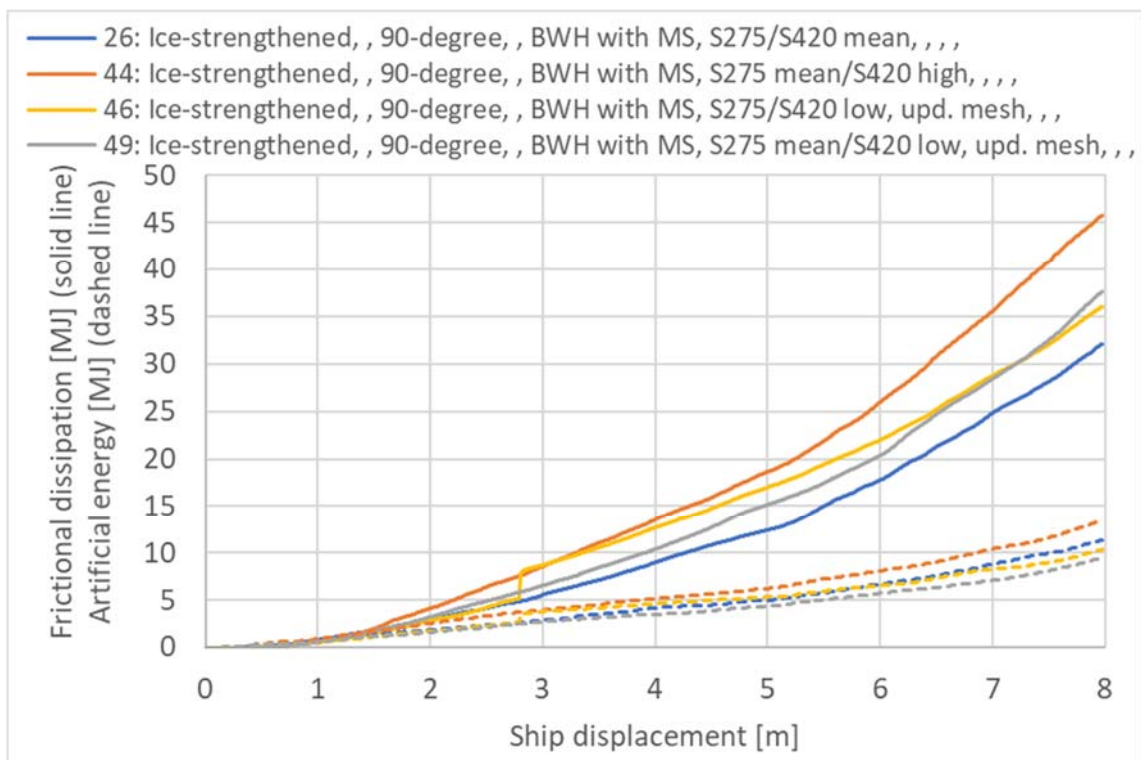


> Figure 3-6 Frictional dissipation and artificial energy [MJ] impact ice-strengthened bow-pontoon 90-degree, sensitivity of material parameters

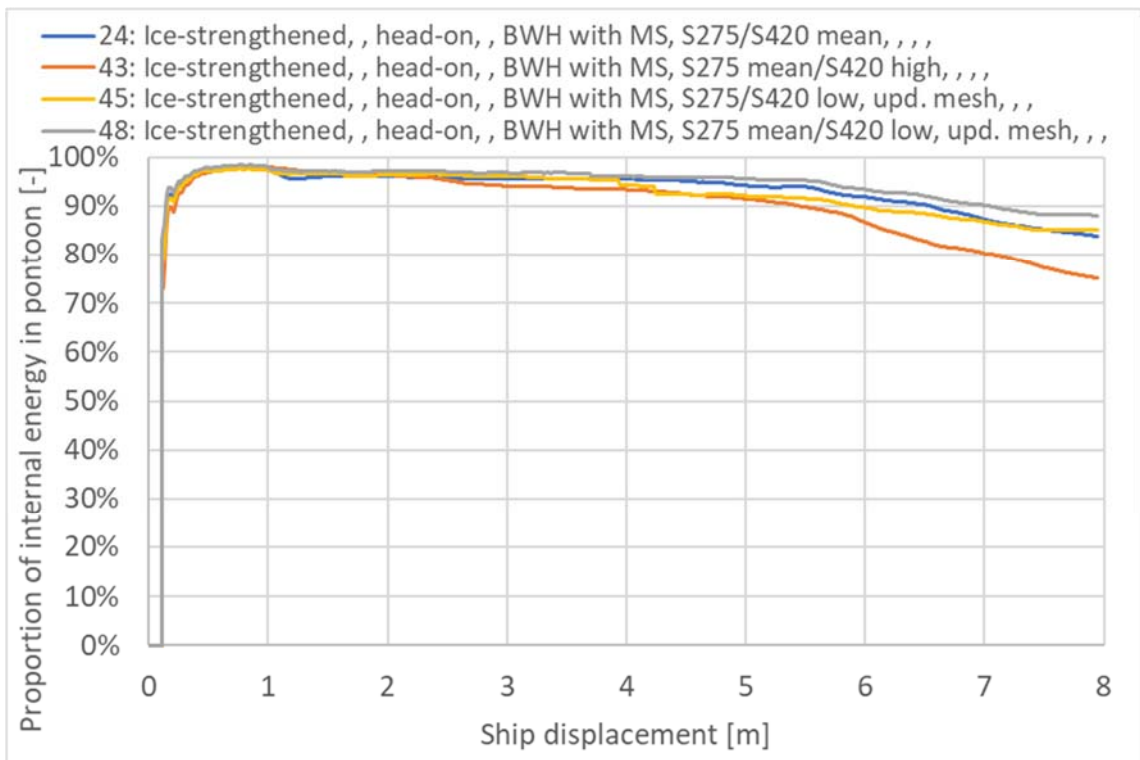


> Figure 3-7 Proportion of internal energy in pontoon [-] impact ice-strengthened bow-pontoon head-on, sensitivity of material parameters

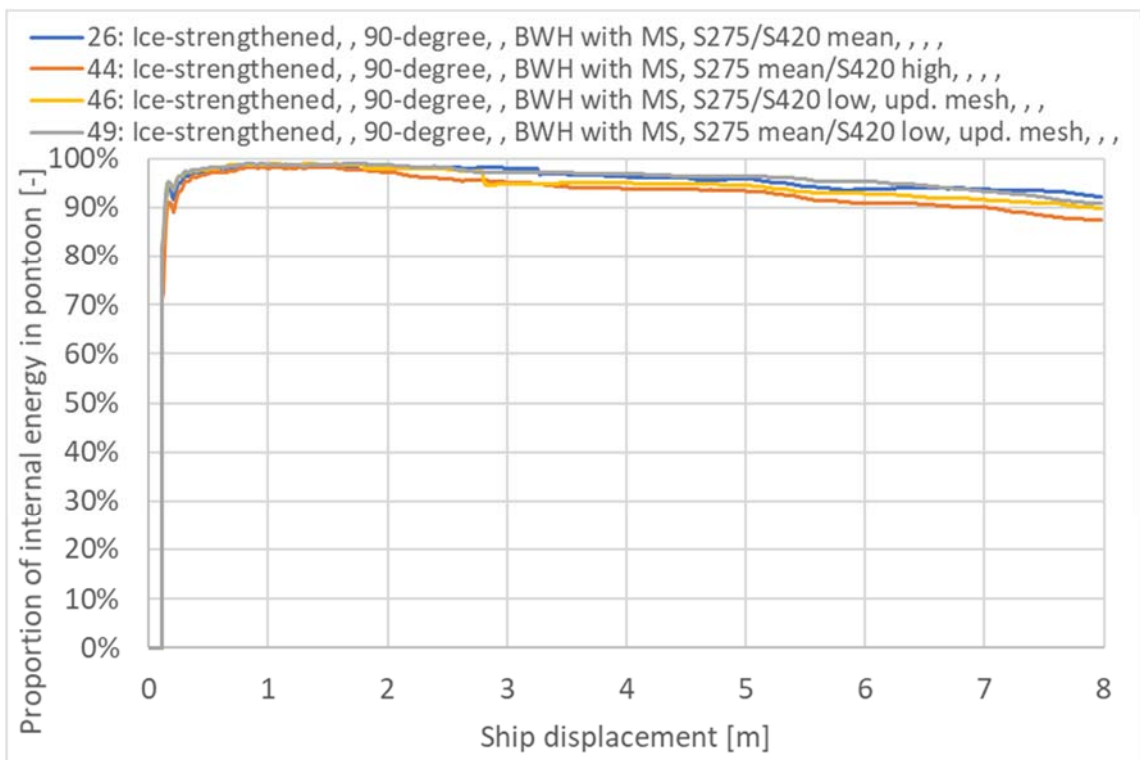


> Figure 3-8 Proportion of internal energy in pontoon [-] impact ice-strengthened bow-pontoon 90-degree, sensitivity of material parameters

Figure 3-9 shows a graphical presentation of the sensitivity of the material parameters investigated for impact with the ice-strengthened bow. The maximum force from Figure 3-1 and Figure 3-2 is plotted, defined by a cut-off at ship displacement corresponding 100 MJ for the respective simulation.

The simulations with the ice-strengthened bow are not that sensitive to the "mean-high" set of material parameters as seen for the container bow impact simulations in section 2. Impact between bulkheads and frames gives as expected large displacement before the same energy level is obtained. This impact also results in a relatively high maximum impact force which occurs at a later stage of the impact, see [1] Figure 5-15.

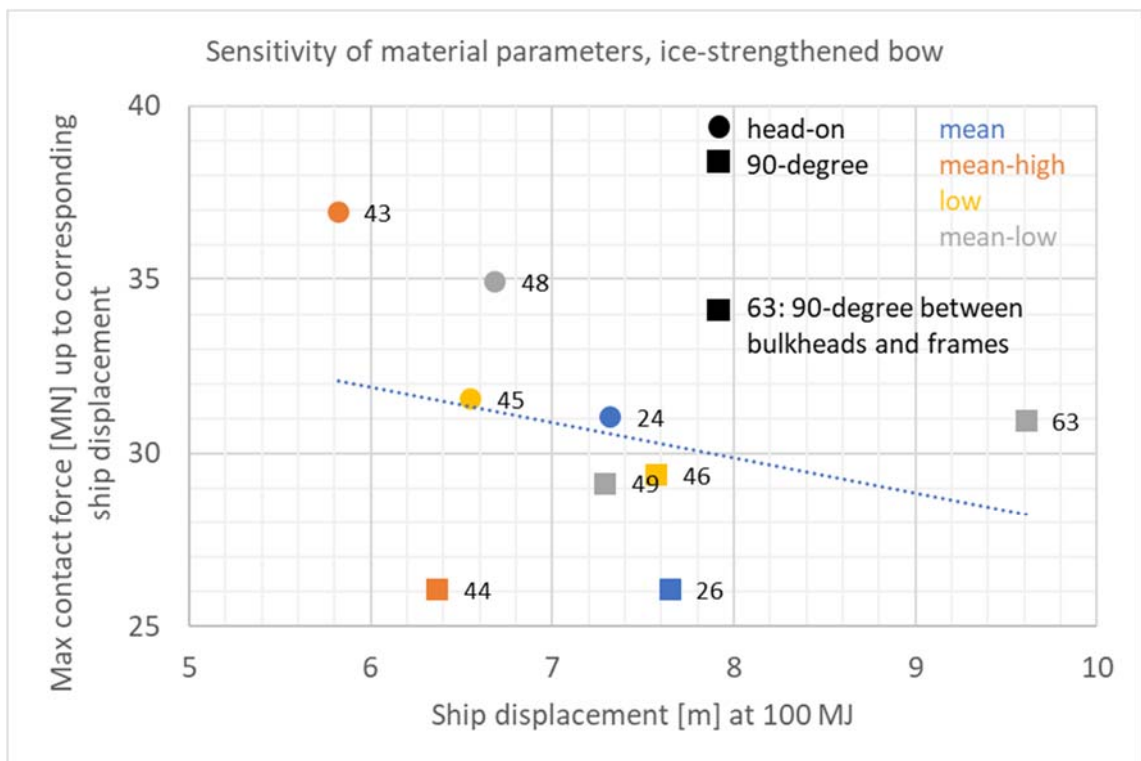


> Figure 3-9 Sensitivity of material parameters, impact ice-strengthened bow-pontoon

4 SENSITIVITY OF MATERIAL DAMAGE MODELS

This section investigates the sensitivity of material damage models. Three sets of analysis have been conducted, which have also been investigated in Appendix B [5].

- BWH model without mesh scaling
- BWH model with mesh scaling
- FLD material model with Swift instability (only for the container bow)

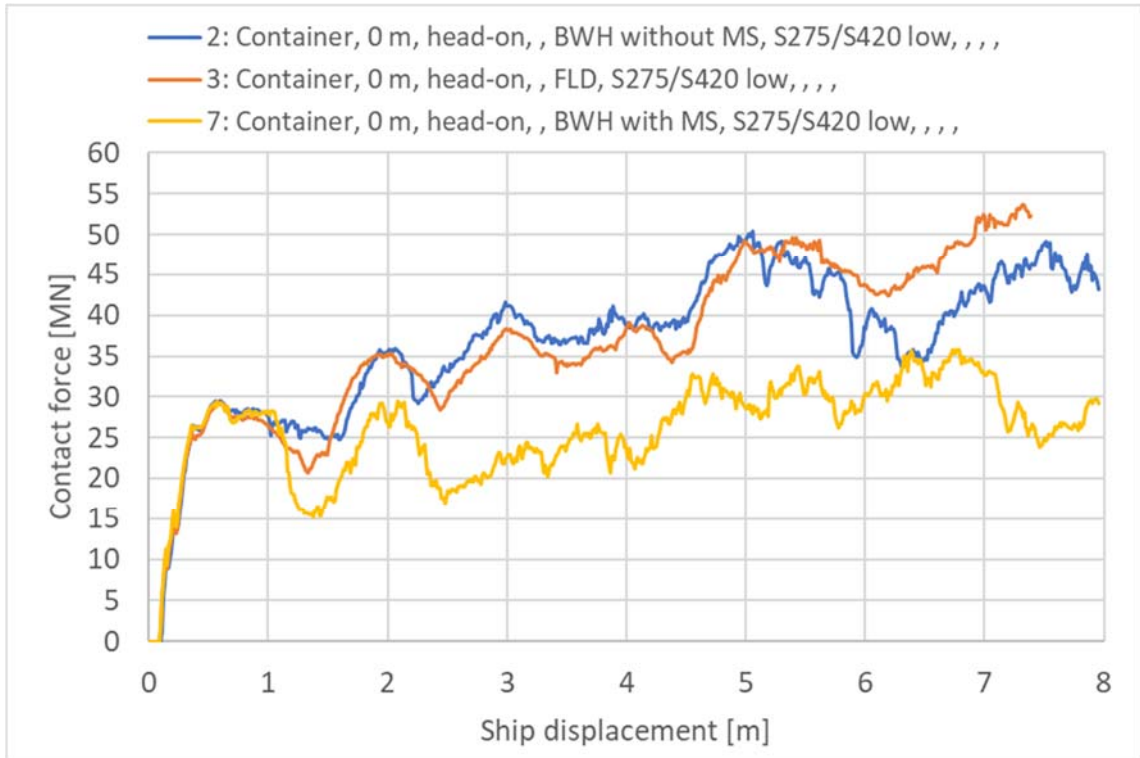
For discussion about the different material damage models, see chapter 3 [1] and Appendix B [5].

Figure 4-1 and Figure 4-2 show the resulting force-displacement curves. The FLD material display similar results as the BWH model without mesh scaling. The BWH model with mesh scaling displays lower force level than the two other models, which is expected.

With reference to the sensitivity model reported in section 3.4.2 [1] the difference in force level is more significant in simulations using the BWH model without mesh scaling than for the simulations where mesh scaling is applied. Since the results for length/thickness (l/t)-ratio=1 without mesh scaling is in the same range as results with mesh scaling and l/t -ratio of 1-25, the full analysis is run utilizing the BWH model with mesh scaling applied to the entire model. The characteristic element length is 100-150 mm for the ship bows and 100 mm for the pontoon, giving l/t -ratio of approximately 5-15.

Note that the initial impact is almost identical with the different material damage model, which is also seen for the sensitivity model reported in Appendix B section 2 [5].

ID-no.	Max. contact force [MN] 0-4 m	Mean contact force [MN] 0-4 m
2	42	32
3	39	31
7	29	23



> Figure 4-1 Contact force [MN] impact container bow-pontoon, sensitivity of material damage models

ID-no.	Max. contact force [MN] 0-4 m	Mean contact force [MN] 0-4 m
22	25	16
23	18	11

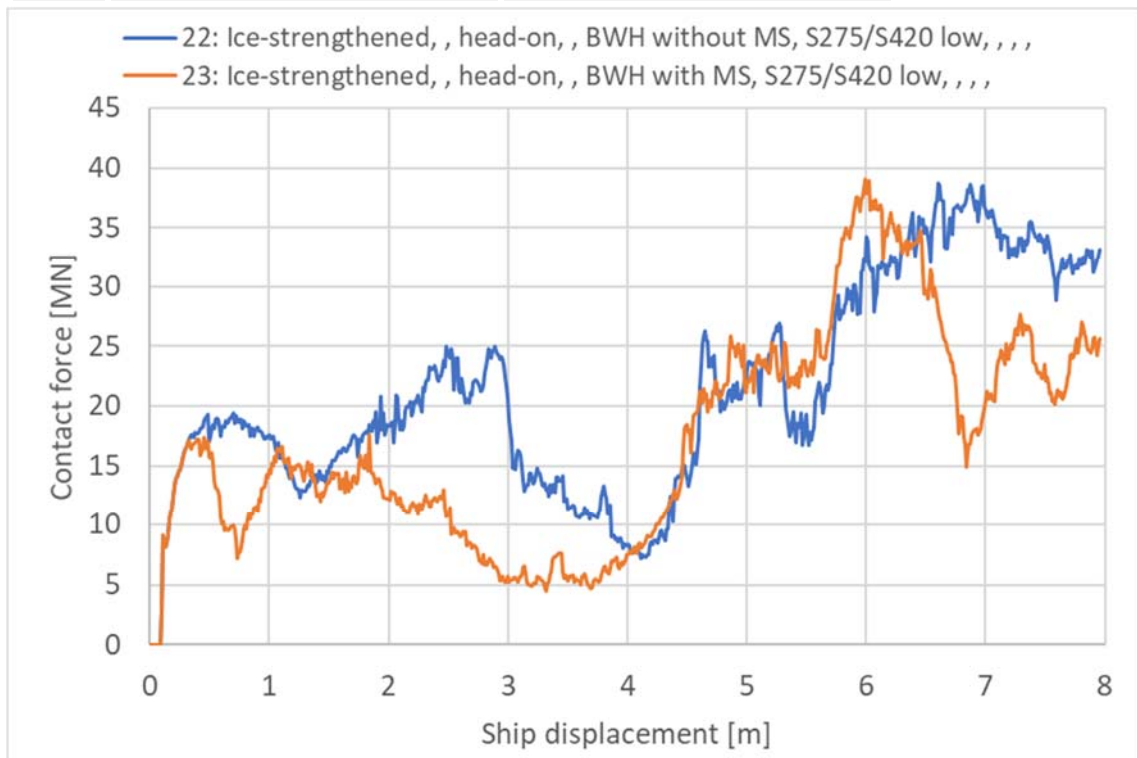
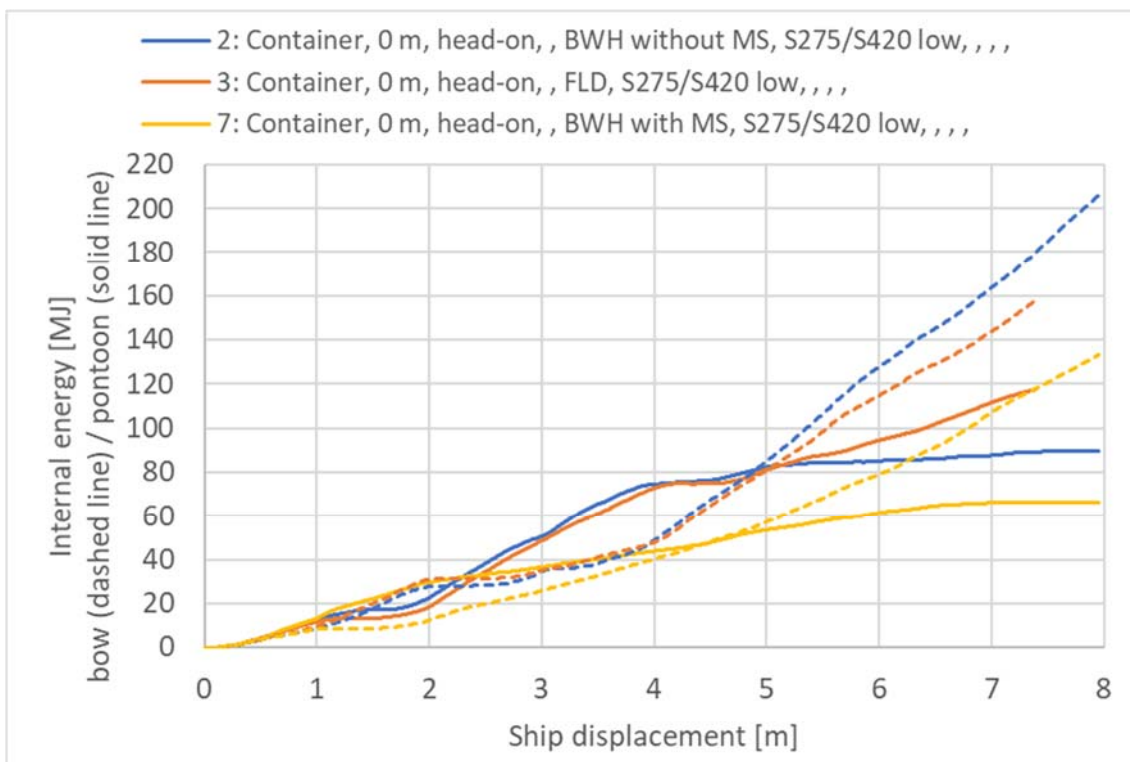


> Figure 4-2 Contact force [MN] impact ice-strengthened bow-pontoon, sensitivity of material damage models

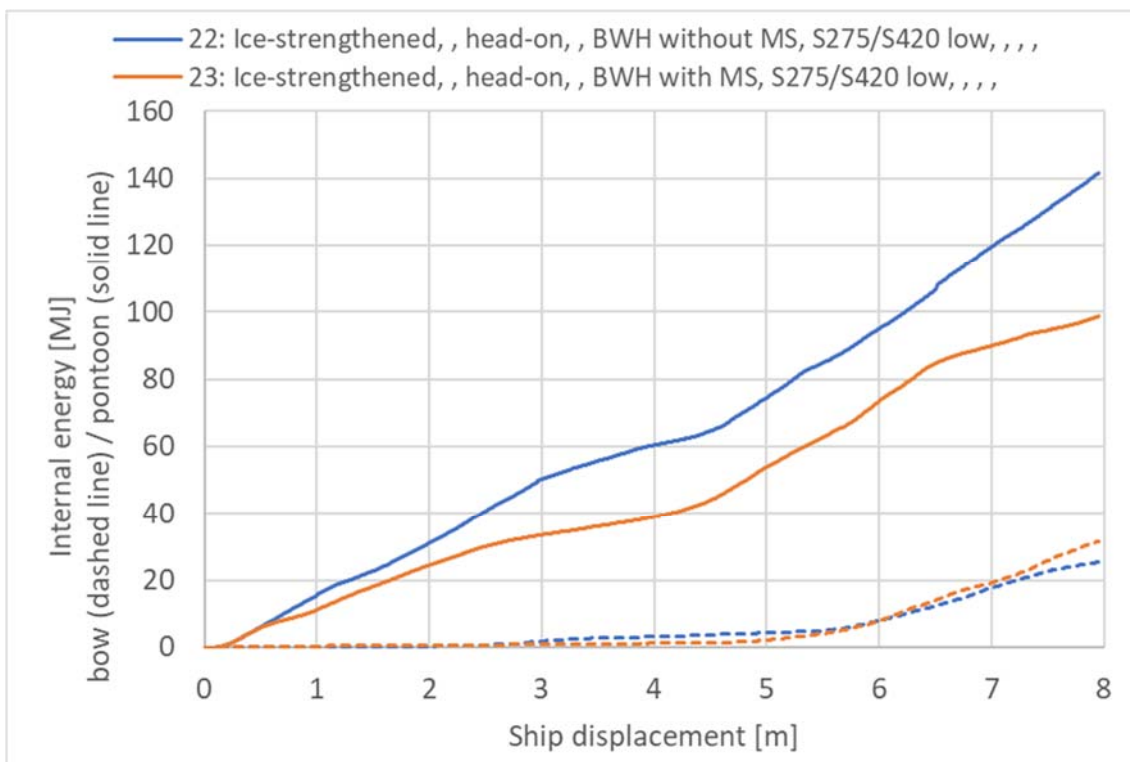
Figure 4-3 and Figure 4-4 show the internal energy dissipated in the bow with dashed line and the pontoon with solid line. The dissipated energy in the container bow is higher than the previous results shown in section 5.3 [1] and section 1 and 2. This is because sensitivity of the material damage models was investigated with impact at scantling height of the container bow. The sensitivity of impact height is explored in section 5.

Figure 4-5 and Figure 4-6 show the frictional dissipation and artificial energy in the models. The proportion of artificial to internal energy is 11-14 % for the displayed models. The artificial energy is particularly high for impact with the container bow utilizing BWH model without mesh scaling.

Figure 4-7 and Figure 4-8 show the proportion of internal energy dissipated in the pontoon. The material damage model does not affect the amount of energy dissipated in the pontoon much. However, the dissipated energy in the pontoon is low for the container bow because the impact height used is the scantling draught and not the design draught. Sensitivity of impact height is investigated in section 6.



> Figure 4-3 Internal energy [MJ] impact container bow-pontoon, sensitivity of material damage models



> Figure 4-4 Internal energy [MJ] impact ice-strengthened bow-pontoon, sensitivity of material damage models

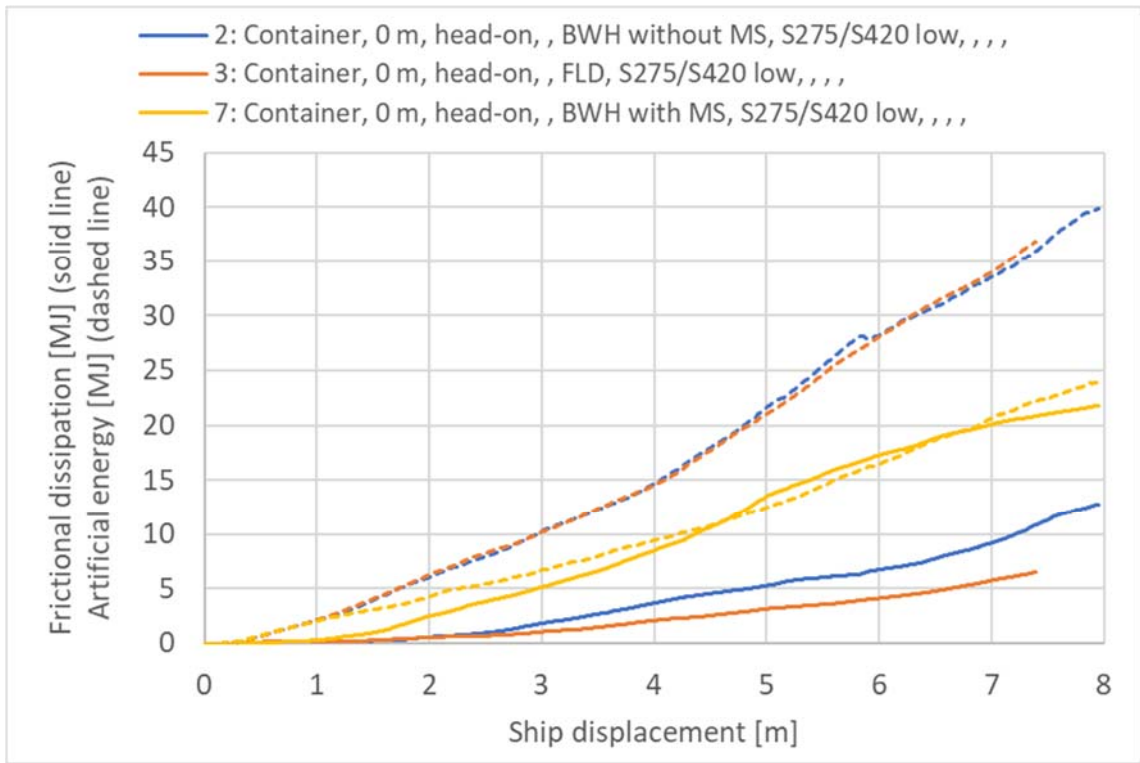


> Figure 4-5 Frictional dissipation and artificial energy [MJ] impact container bow-pontoon, sensitivity of material damage models

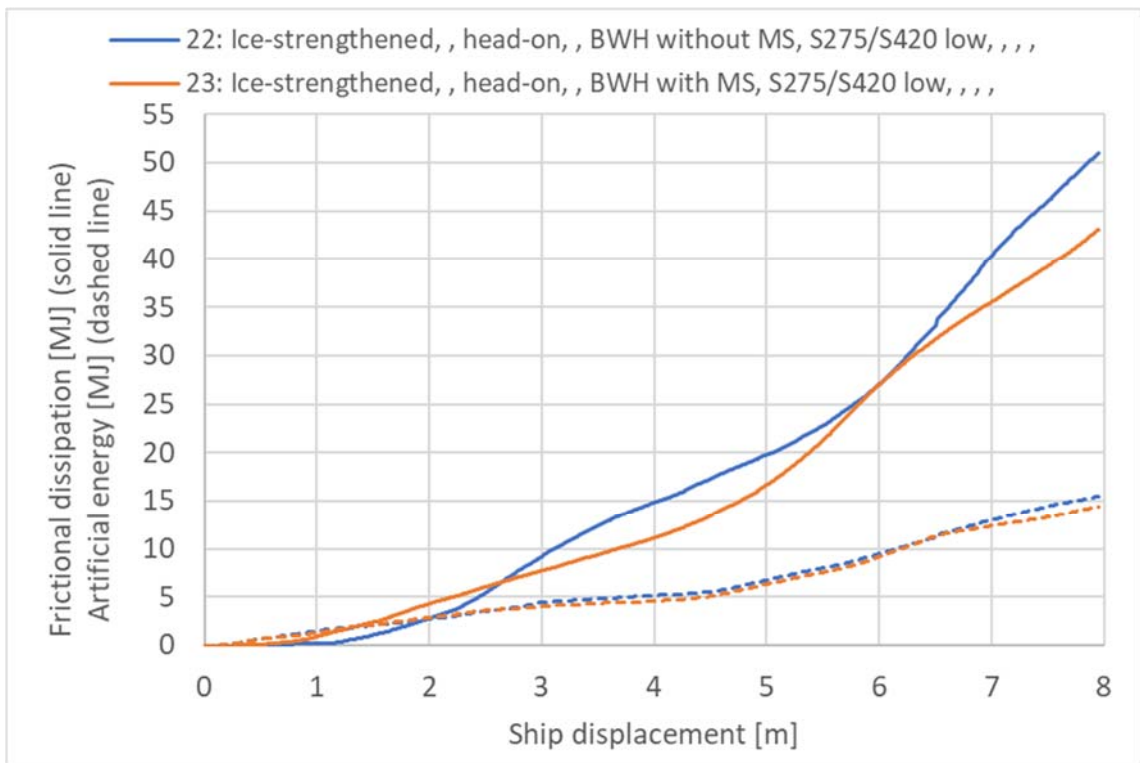


> Figure 4-6 Frictional dissipation and artificial energy [MJ] impact ice-strengthened bow-pontoon, sensitivity of material damage models

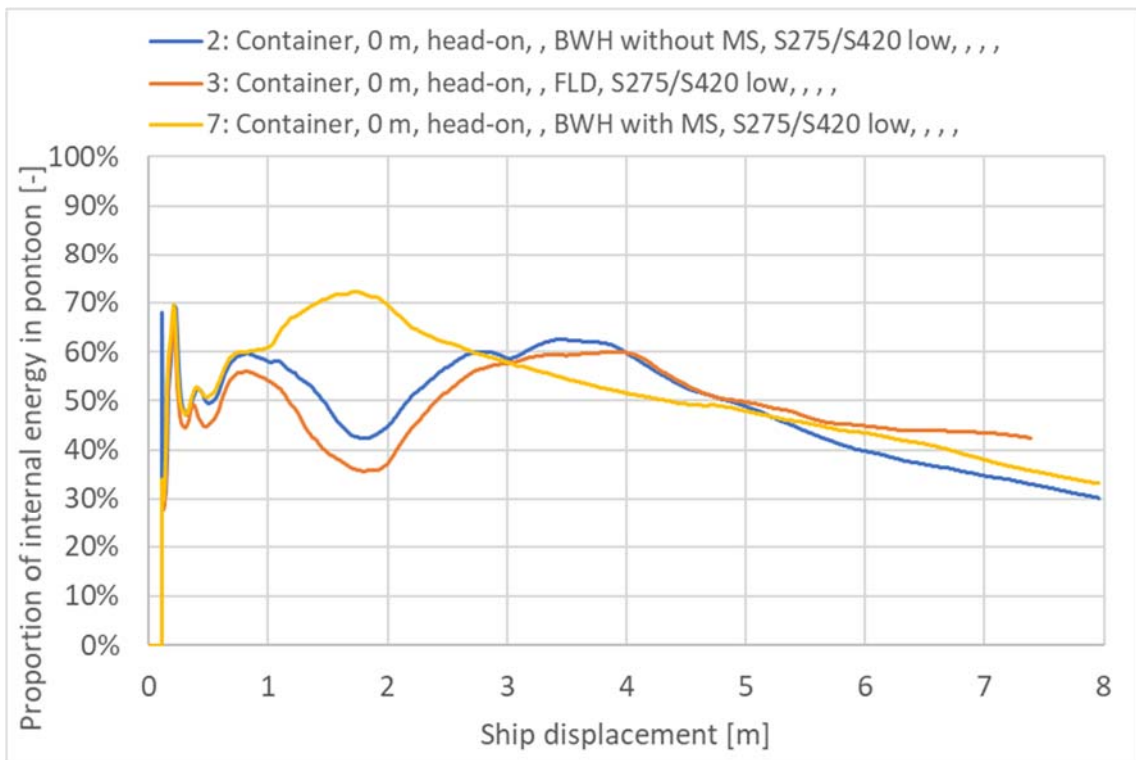


> Figure 4-7 Proportion of internal energy in pontoon [-] impact container bow-pontoon, sensitivity of material damage models

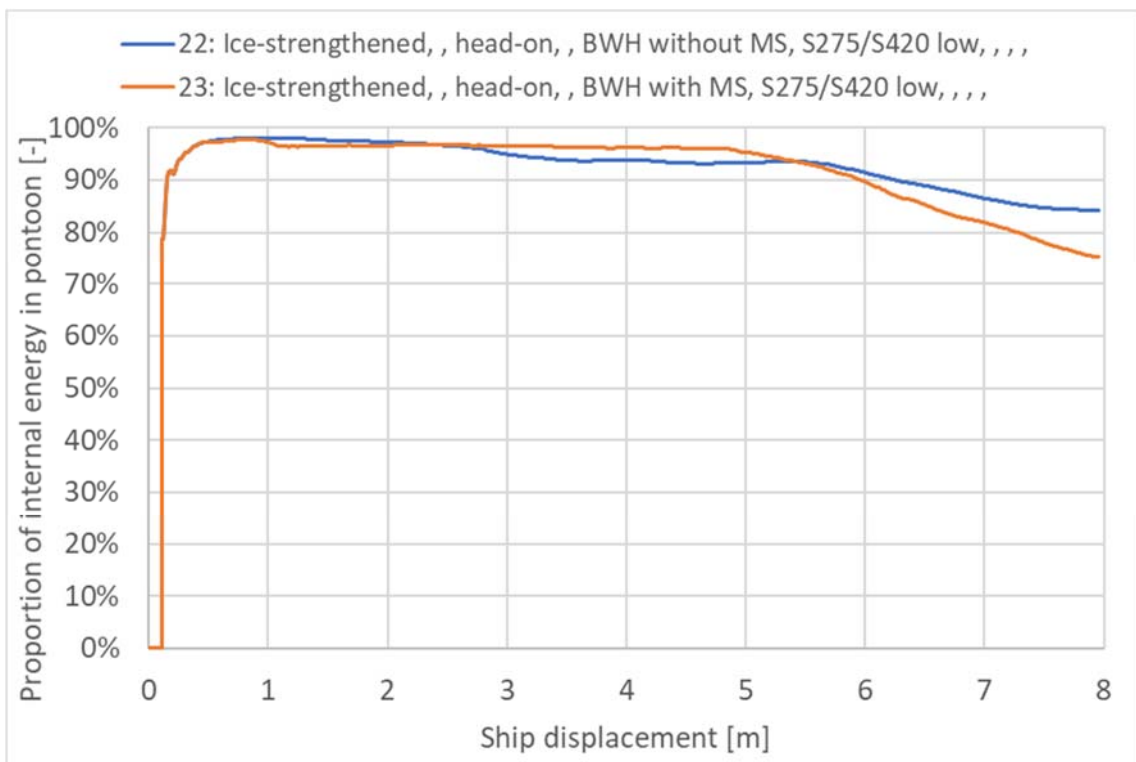


> Figure 4-8 Proportion of internal energy in pontoon [-] impact ice-strengthened bow-pontoon, sensitivity of material damage models

Figure 4-9 shows a graphical presentation of the sensitivity of the material damage models investigated. The maximum force from Figure 4-1 and Figure 4-2 is plotted, defined by a cut-off at ship displacement corresponding 100 MJ for the respective simulation.

The simulation is sensitive to the material damage model utilized. The material damage model utilized is mainly the BWH model with mesh scaling because the finite element model behaves more independently of the mesh size when mesh scaling is applied.

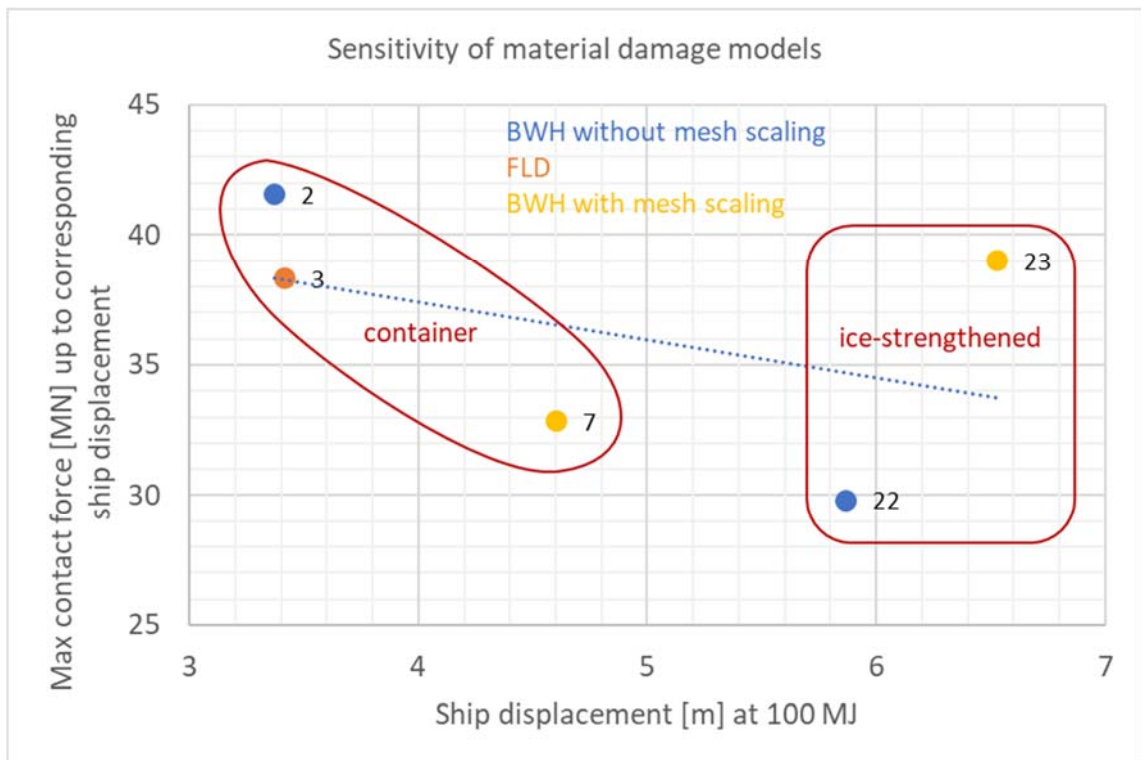


> Figure 4-9 Sensitivity of material damage models

5 SENSITIVITY OF MESH SIZE AND ELEMENT TYPE

This section investigates the sensitivity of mesh size and element type. The sensitivity is checked for the container bow.

Figure 5-1 shows the force-displacement curves for impact with BWH model with and without mesh scaling and for mesh size 100 mm (standard) and 50 mm. The difference in force level is a bit larger between the simulations using material without mesh scaling than for the two simulations where mesh scaling is applied. The results comply to the results in section 3.4.2 [1], but not that well defined. This is because the mesh size has not been varied to the same extent as the sensitivity model reported in section 3.4.2 [1].

When studying the internal energy of the mesh sensitivity models in Figure 5-2, the impact with BWH model without mesh scaling and coarse mesh reveals a significantly higher energy dissipation in the bow than the rest of the models. When mesh scaling is applied, the amount of dissipated energy in the bow and pontoon seems more independent of the mesh size. Deviant results for the BWH model without mesh scaling and coarse mesh is also seen for the frictional dissipation and artificial energy in Figure 5-3.

Figure 5-4 shows that the proportion of internal energy dissipated in the pontoon is low for the BWH model without mesh scaling and mesh size 100 mm. This model deviates from the other models and confirms that the BWH model without mesh scaling is mesh sensitive. The BWH model without mesh scaling with 50 mm mesh size display similar proportion of energy dissipation in the pontoon as the other models.

The 100 mm mesh size for the pontoon is considered sufficiently fine when utilizing mesh scaling of the BWH model. 100 mm mesh size is also equal to the orphan mesh size of the ship models. Smaller elements result in lower contact force, and 100 mm mesh is thus conservative.

ID-no.	Max. contact force [MN] 0-4 m	Mean contact force [MN] 0-4 m
5	49	35
6	41	28
10	36	26
12	32	21

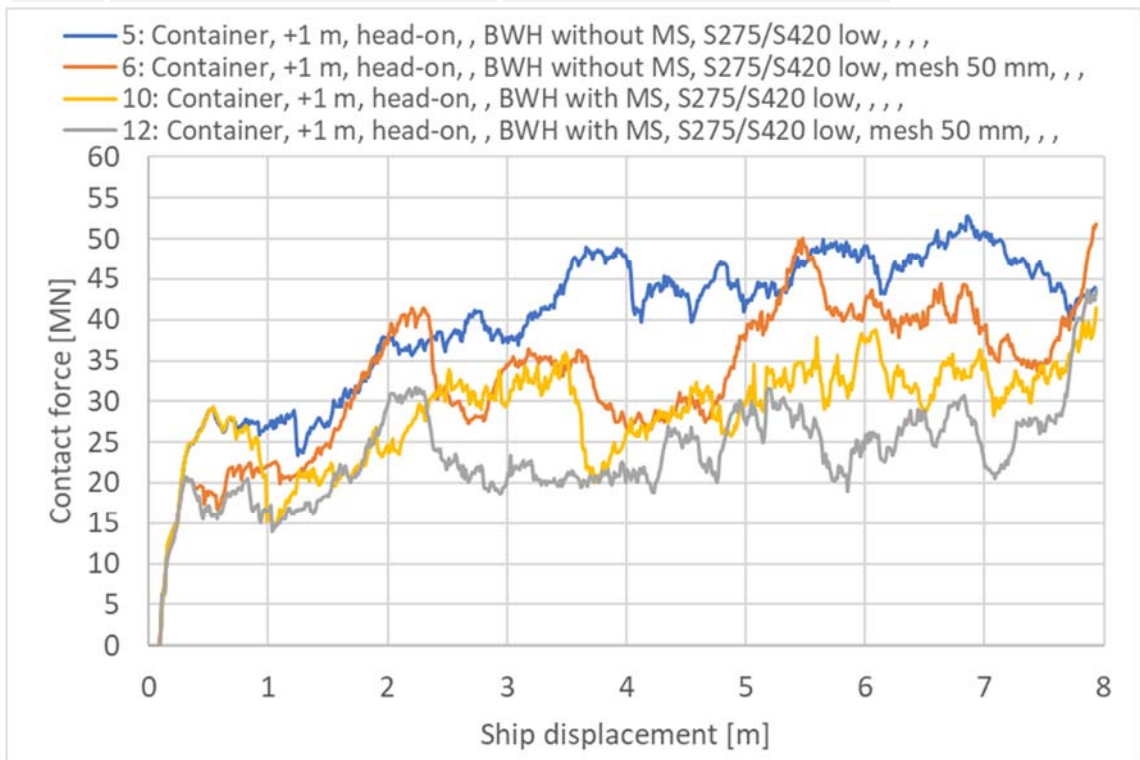


> Figure 5-1 Contact force [MN] impact bow-pontoon, sensitivity of mesh size

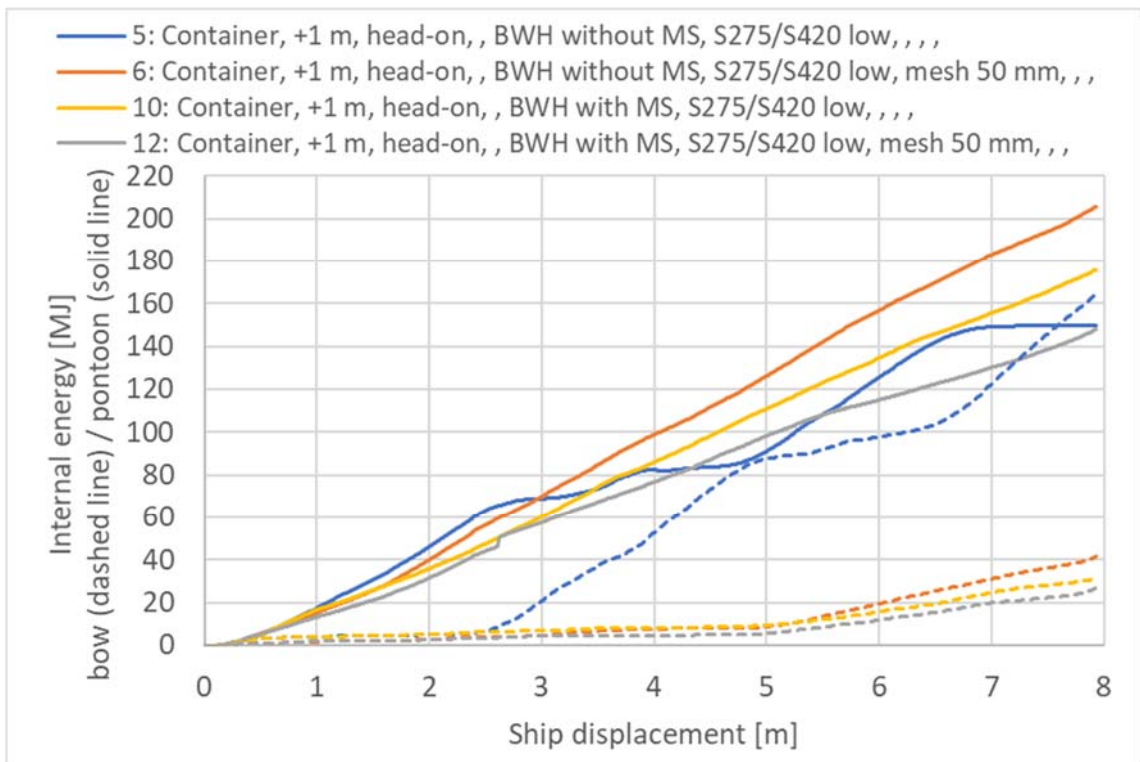


> Figure 5-2 Internal energy [MJ] impact bow-pontoon, sensitivity of mesh size

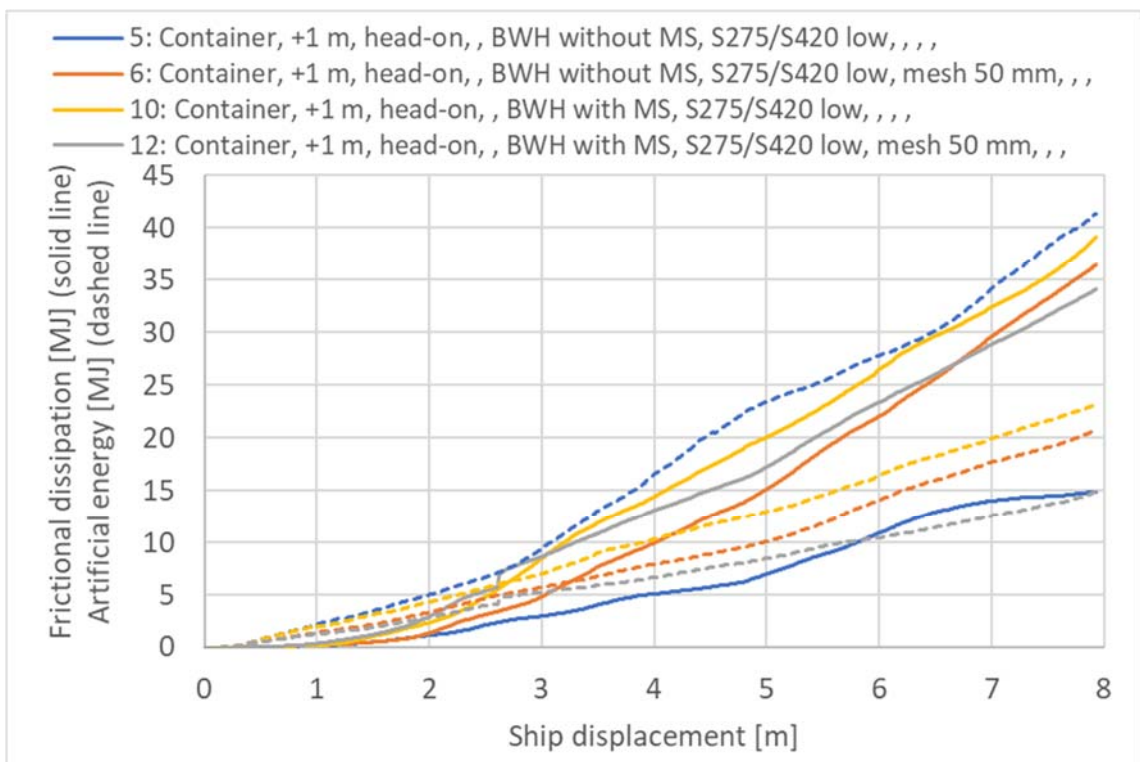


> Figure 5-3 Frictional dissipation and artificial energy [MJ] impact bow-pontoon, sensitivity of mesh size

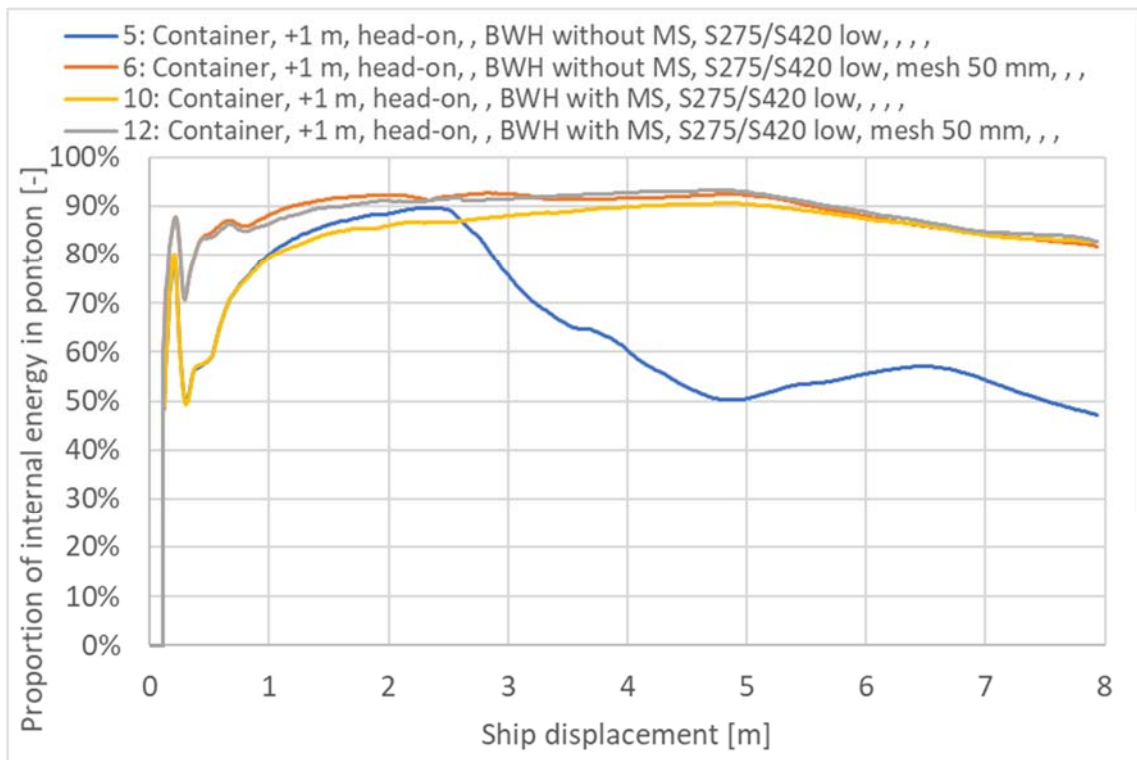


> Figure 5-4 Proportion of internal energy in pontoon [-] impact bow-pontoon, sensitivity of mesh size

Figure 5-5 shows the force-displacement curves for simulation with full (S4 elements) or reduced (S4R elements) integration of the elements. Except for the first peak, full integration generally displays lower force level. This follows the results in Appendix B section 3 [5]. A higher force level is generally conservative when studying ship impact for global assessment, see [6], justifying the results with reduced integration.

Figure 5-6 shows also higher dissipated energy in the bow when full integration is conducted. The difference may be due to the first peak in the force-displacement curve which triggers the following impact scenario to crush the bow more and the pontoon less than observed for the model with reduced integration. This is not an expected behavior. Figure 5-8 also reflects the changed energy dissipation behavior. However, it may be concluded that employing reduced integration is on the safe side with regards to local damage evaluation of the pontoon.

Artificial energy is significantly lower for the model with full integration as shown in Figure 5-7, which is expected. Of all simulations conducted, only two models display low artificial energy; the one with full integration and the one with impact between bulkheads and frames instead of directly on a bulkhead. See Figure 5-9.

Other hourglass formulations have been tested to try to reduce the artificial energy, but the default formulation gave the lowest artificial energy. The Abaqus documentation [7] discourages to increase the default hourglass stiffness, but recommends to rather reduce the element size to avoid the hourglass modes and thus reduce the artificial energy. The two models with 50 mm mesh size displayed lower proportion of artificial energy than their reference models with 100 mm mesh size, but the mesh needs to be refined even more to achieve a larger reduction to the artificial energy. All these attempts to reduce the artificial

energy is with the cost of computational time. Full integration increases the computational time with a factor of 3, and to halve the element size increases the computational time with a factor of 3.5.

ID-no.	Max. contact force [MN] 0-4 m	Mean contact force [MN] 0-4 m
10	36	26
18	34	21

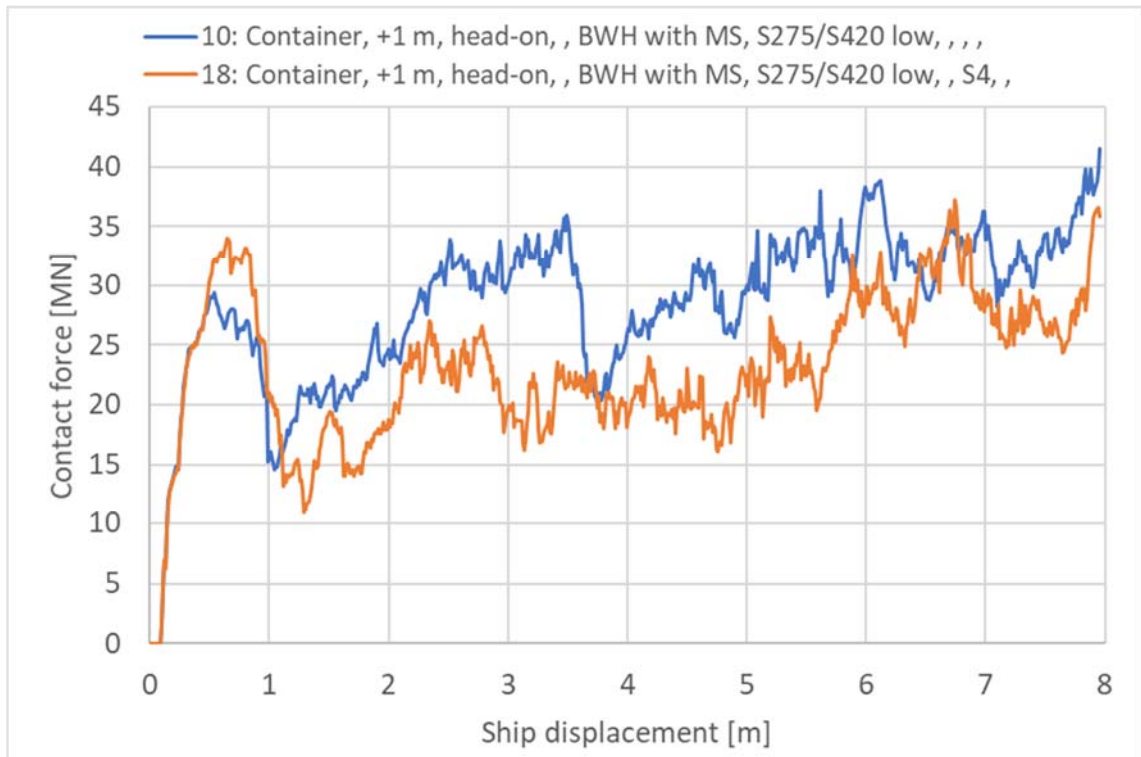


> Figure 5-5 Contact force [MN] impact bow-pontoon, sensitivity of element type

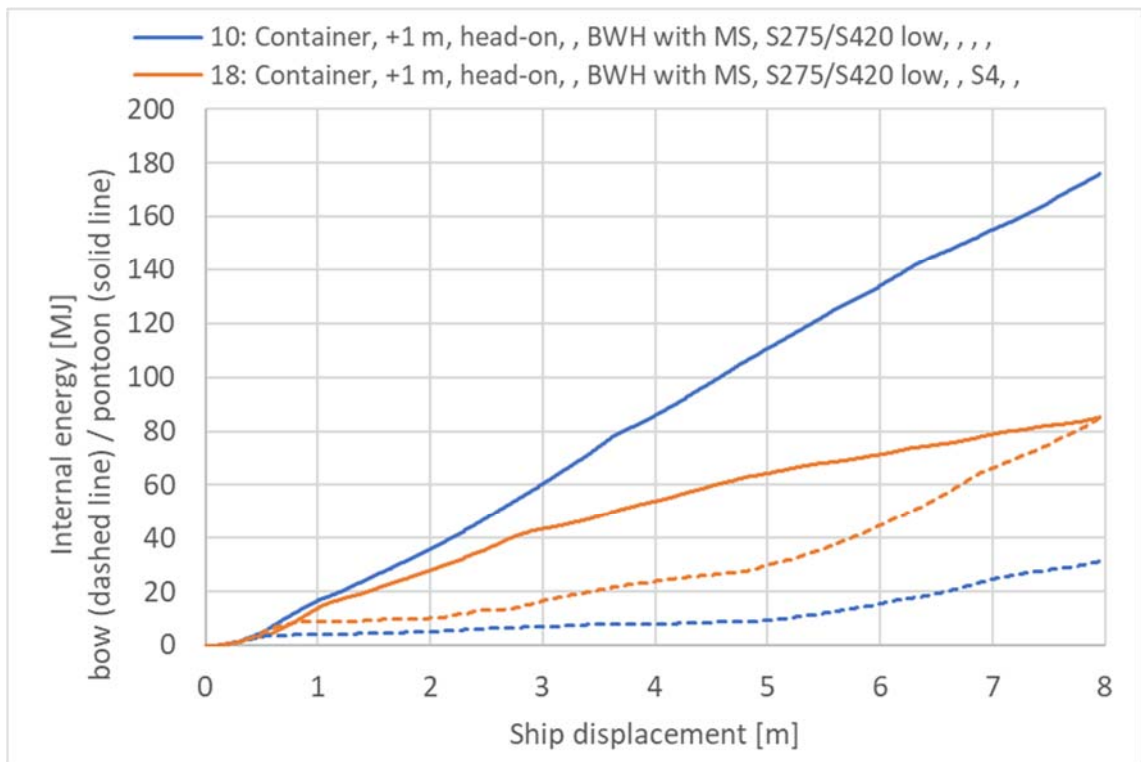


> Figure 5-6 Internal energy [MJ] impact bow-pontoon, sensitivity of element type

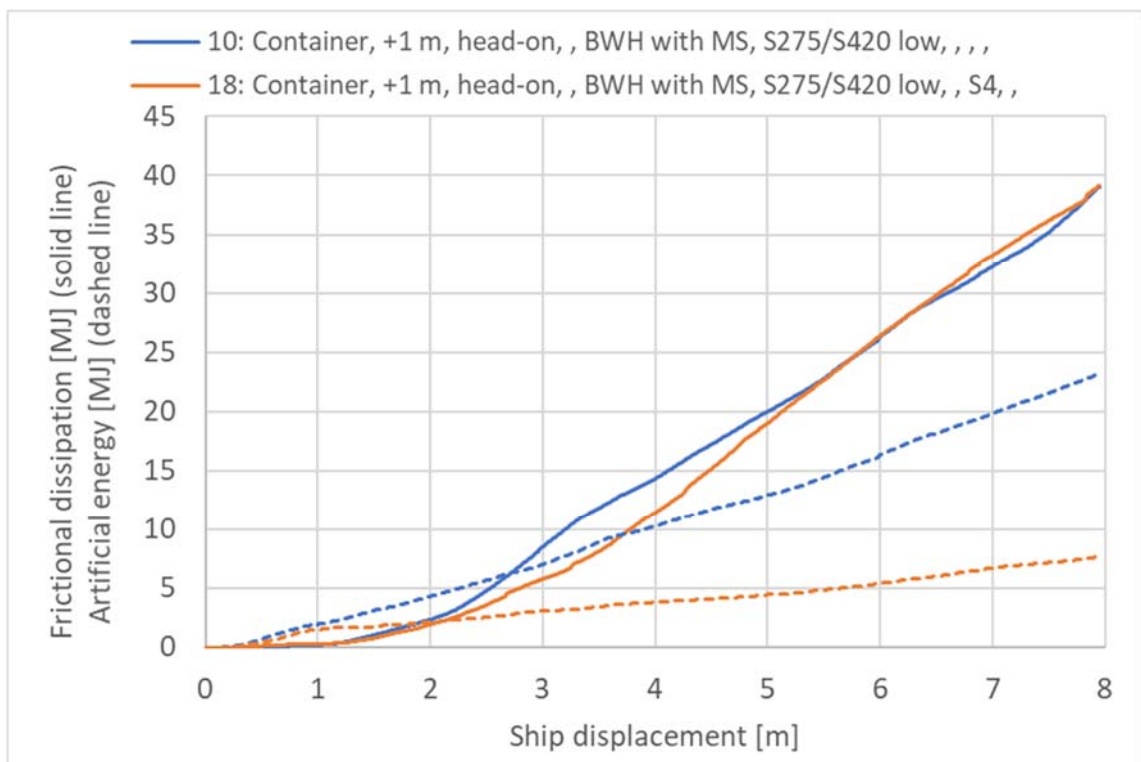


> Figure 5-7 Frictional dissipation and artificial energy [MJ] impact bow-pontoon, sensitivity of element type

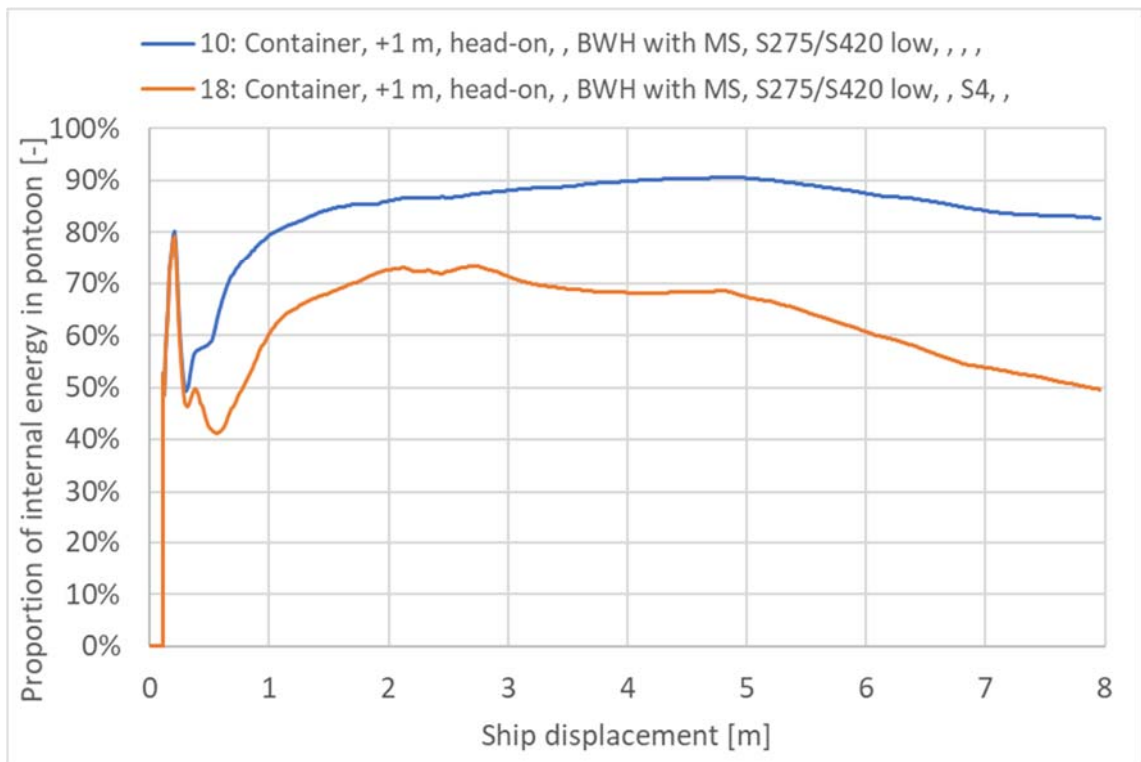
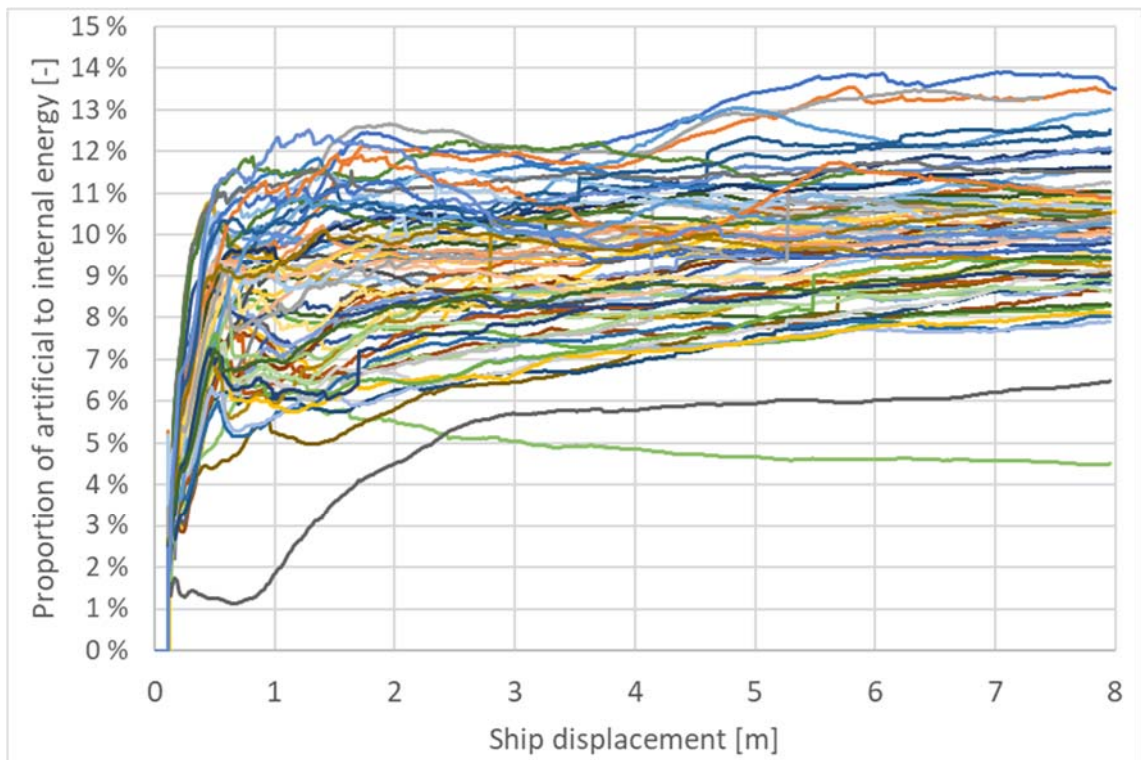


> Figure 5-8 Proportion of internal energy in pontoon [-] impact bow-pontoon, sensitivity of element type



- > *Figure 5-9 Proportion of artificial energy to internal energy [-] impact bow-pontoon: The lowest curve (green) is with full integration, the second lowest curve (grey) is impact 90-degree between bulkheads and frames with reduced integration*

Figure 5-10 shows a graphical presentation of the sensitivity of mesh size and element type investigated. The maximum force from Figure 5-1 and Figure 5-5 is plotted, defined by a cut-off at ship displacement corresponding 100 MJ for the respective simulation.

The simulation is sensitive to the material damage model and element type utilized, more than the mesh size. The material damage model utilized is mainly the BWH model with mesh scaling because the finite element model behaves more independently of the mesh size when mesh scaling is applied.

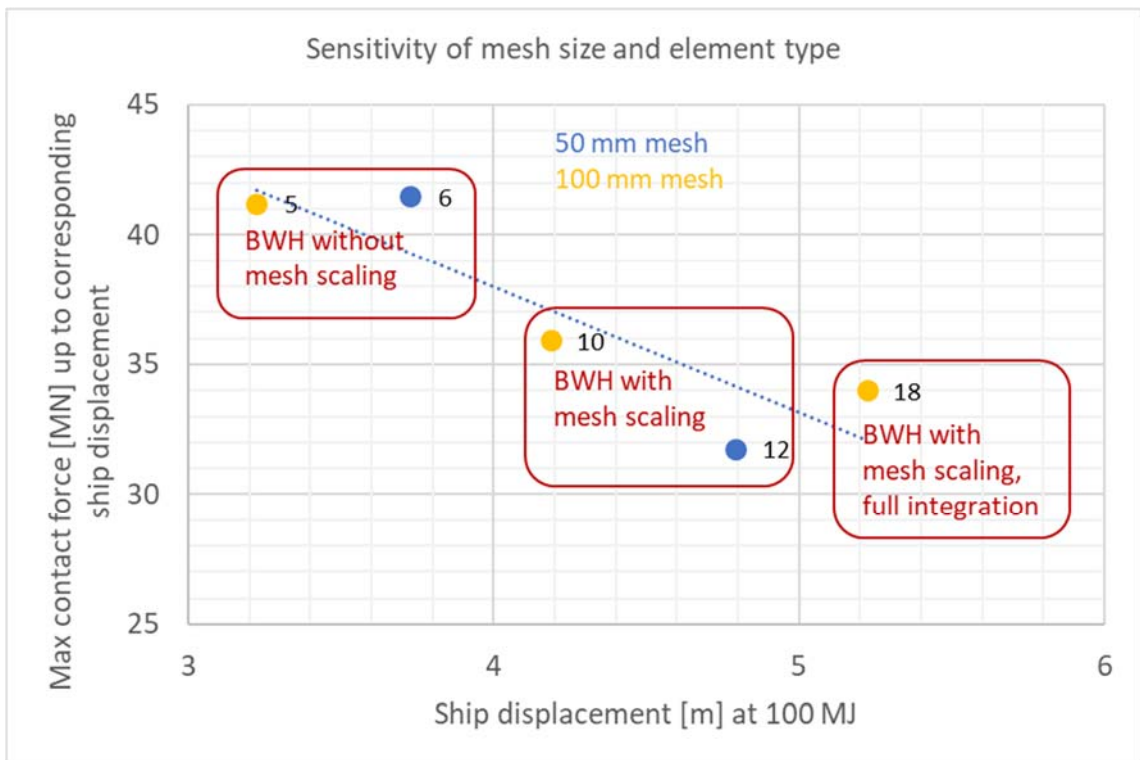


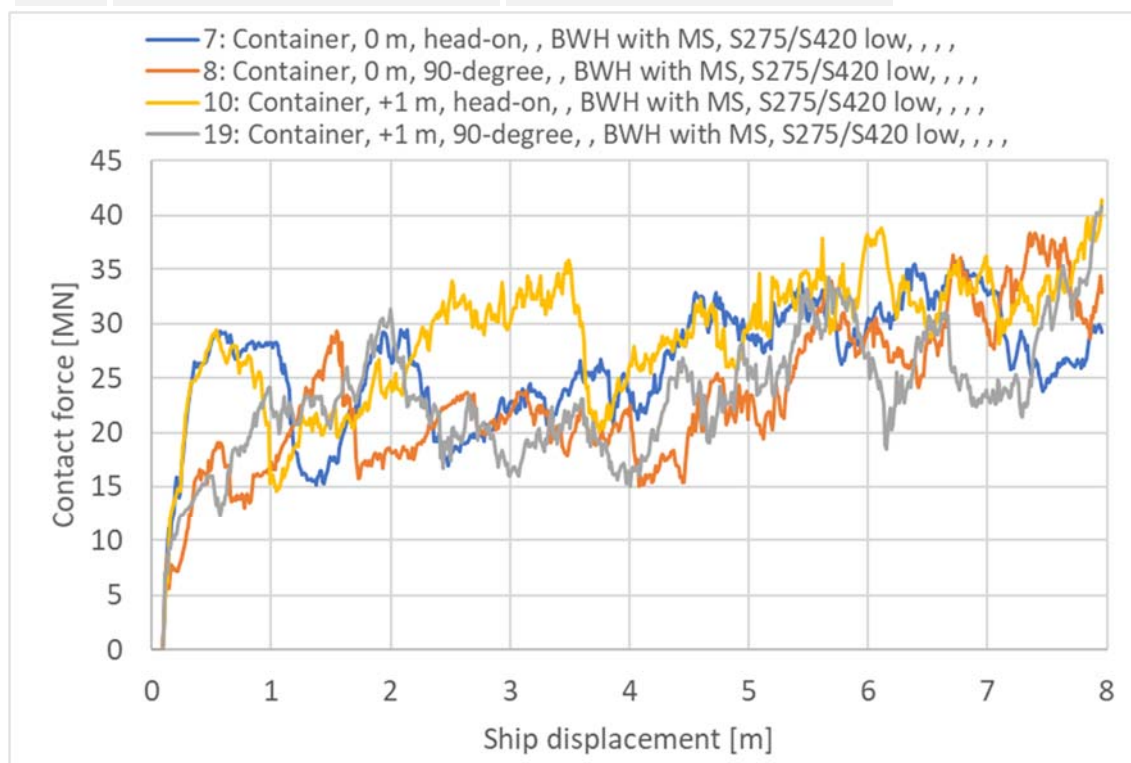
> Figure 5-10 Sensitivity of mesh size and element type

6 SENSITIVITY OF IMPACT HEIGHT AND VELOCITY

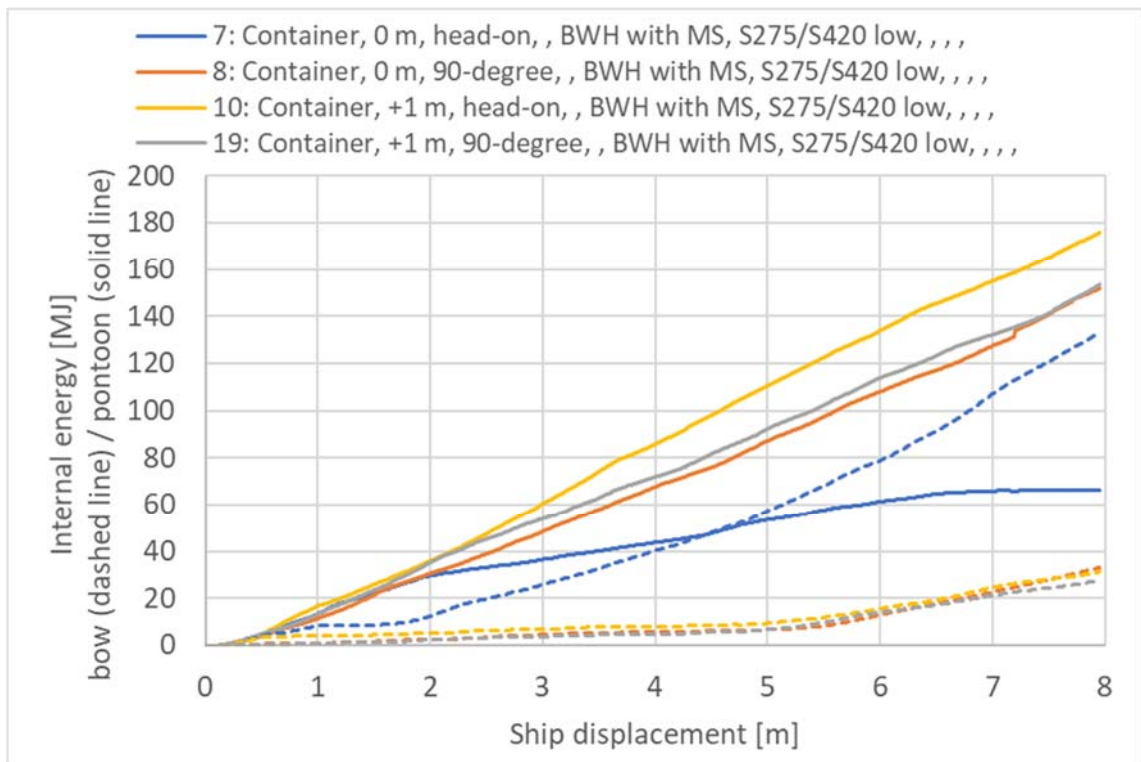
This section investigates the sensitivity of impact height and velocity. The sensitivity is checked for the container bow.

From Figure 6-1, it is seen that impact height at an assumed design draught ("+1.0 m") above the scantling draught ("0 m") results in a bit higher force level. Figure 6-2 shows that the dissipated energy in the bow is significantly higher for the head-on impact at scantling draught, which is also reflected in Figure 6-4 where the proportion of dissipated energy in the pontoon is low. This is a bit surprising, and the container bow is not that sensitive to impact height for the 90-degree impact. It is chosen to use 1.0 m above the scantling draught as the base impact height for the container bow.

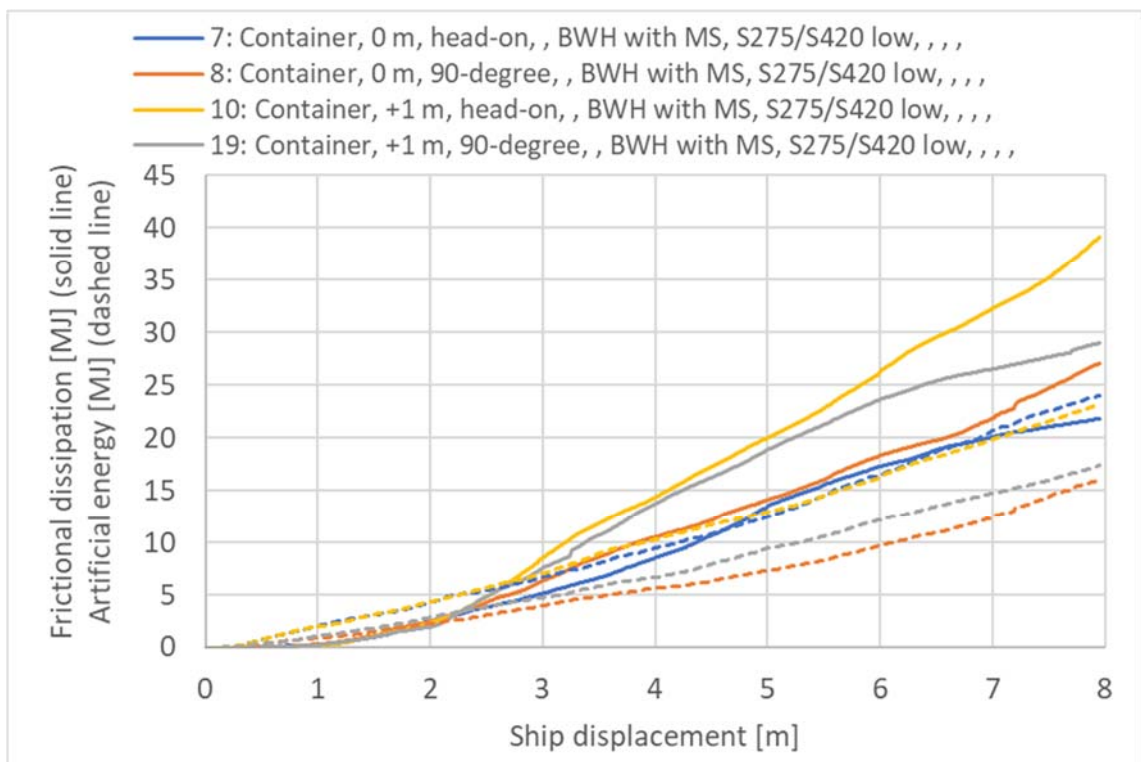
ID-no.	Max. contact force [MN] 0-4 m	Mean contact force [MN] 0-4 m
7	29	23
8	29	19
10	36	26
19	31	20



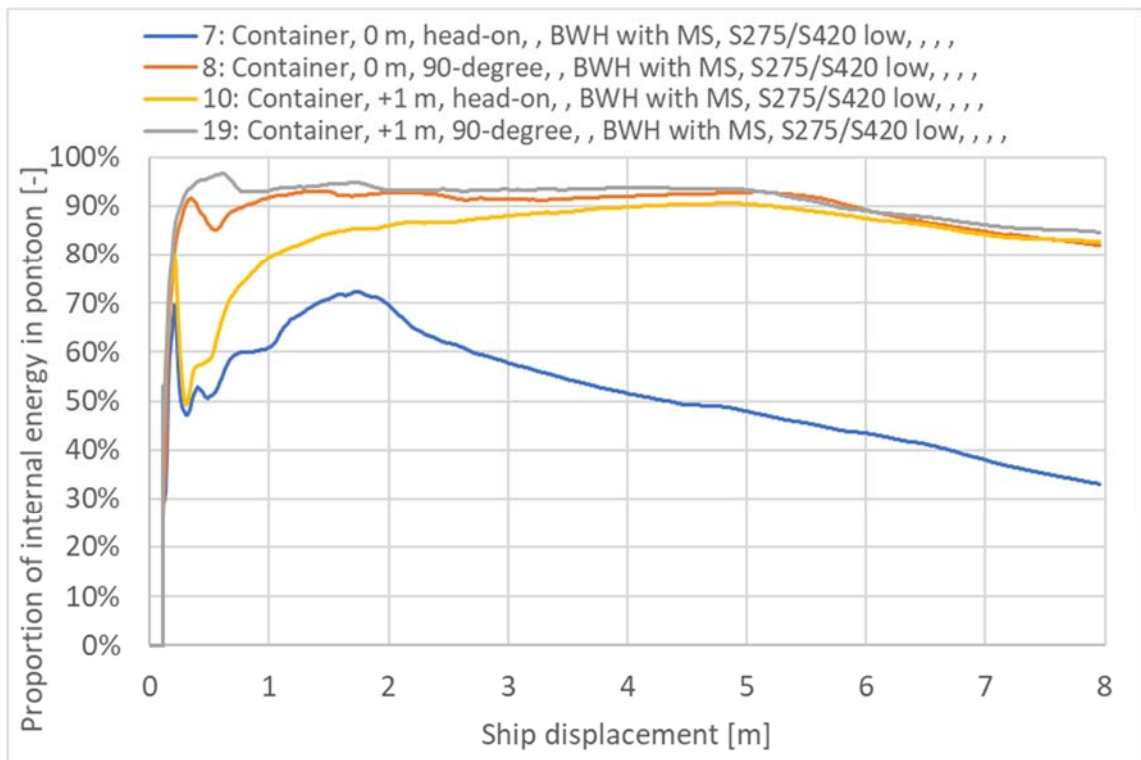
> Figure 6-1 Contact force [MN] impact bow-pontoon, sensitivity of impact height



> Figure 6-2 Internal energy [MJ] impact bow-pontoon, sensitivity of impact height



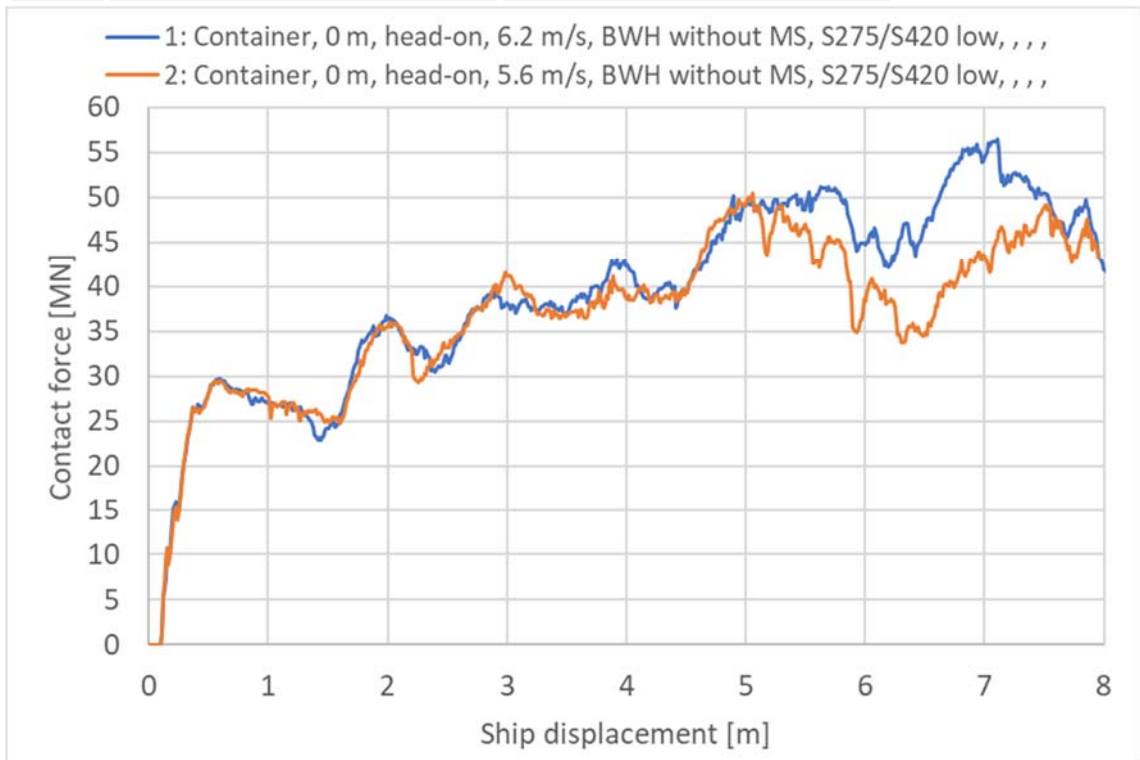
> Figure 6-3 Frictional dissipation and artificial energy [MJ] impact bow-pontoon, sensitivity of impact height



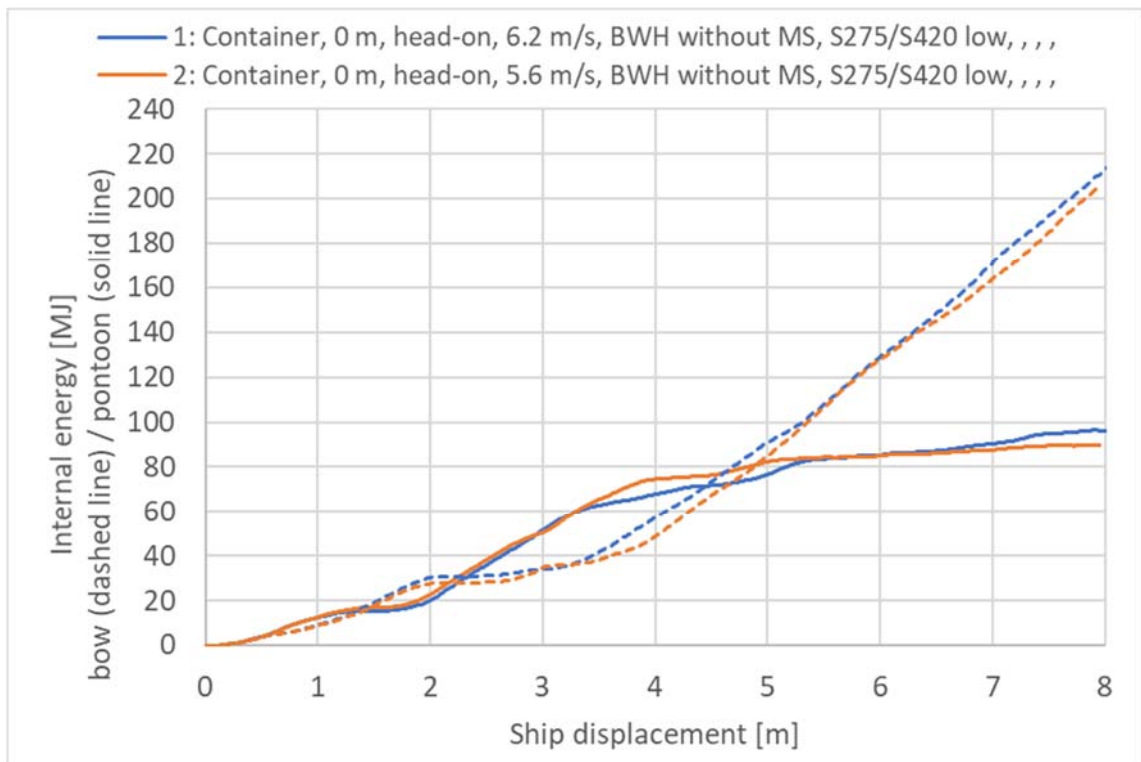
> Figure 6-4 Proportion of internal energy in pontoon [-] impact bow-pontoon, sensitivity of impact height

Figure 6-5 to Figure 6-8 show that the local impact simulation is not very sensitive to a small change of the impact velocity. The Design Basis [8] states that the impact velocity for the pontoon in axis 3 shall be 5.6 m/s for pontoon spacing 100 m and 5.7 m/s for pontoon spacing 125 m.

ID-no.	Max. contact force [MN] 0-4 m	Mean contact force [MN] 0-4 m
1	43	32
2	42	32



> Figure 6-5 Contact force [MN] impact bow-pontoon, sensitivity of velocity



> Figure 6-6 Internal energy [MJ] impact bow-pontoon, sensitivity of velocity

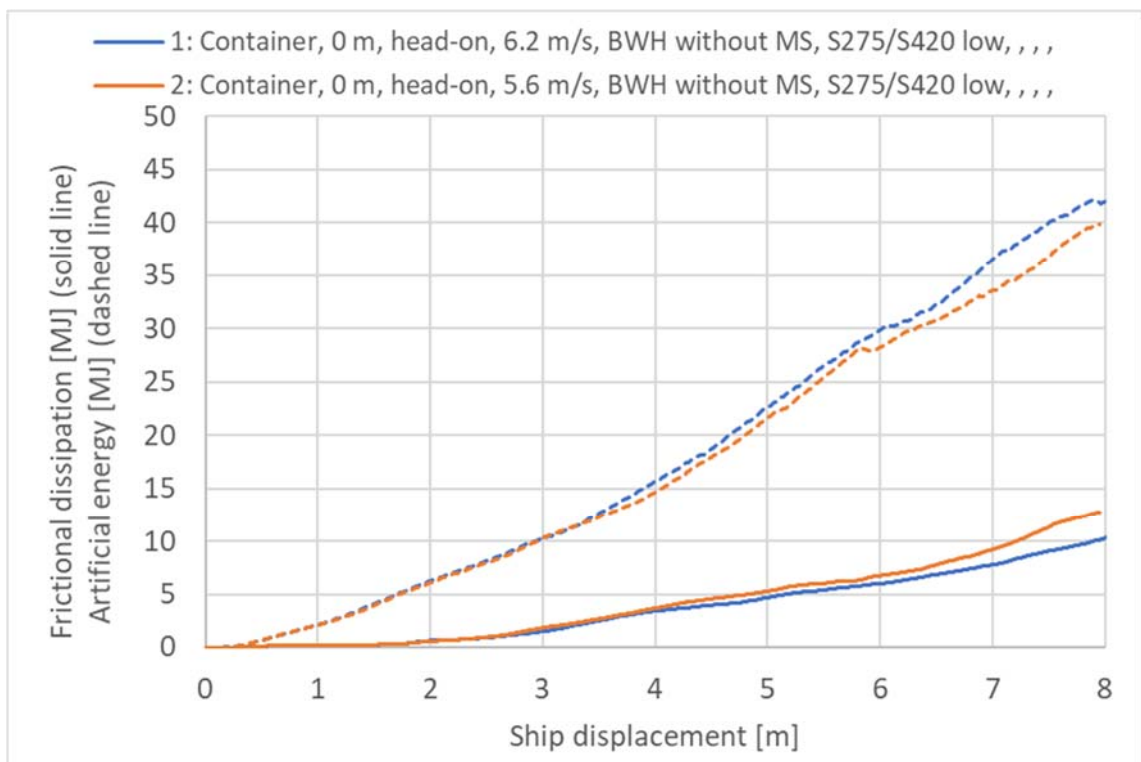


> Figure 6-7 Frictional dissipation and artificial energy [MJ] impact bow-pontoon, sensitivity of velocity

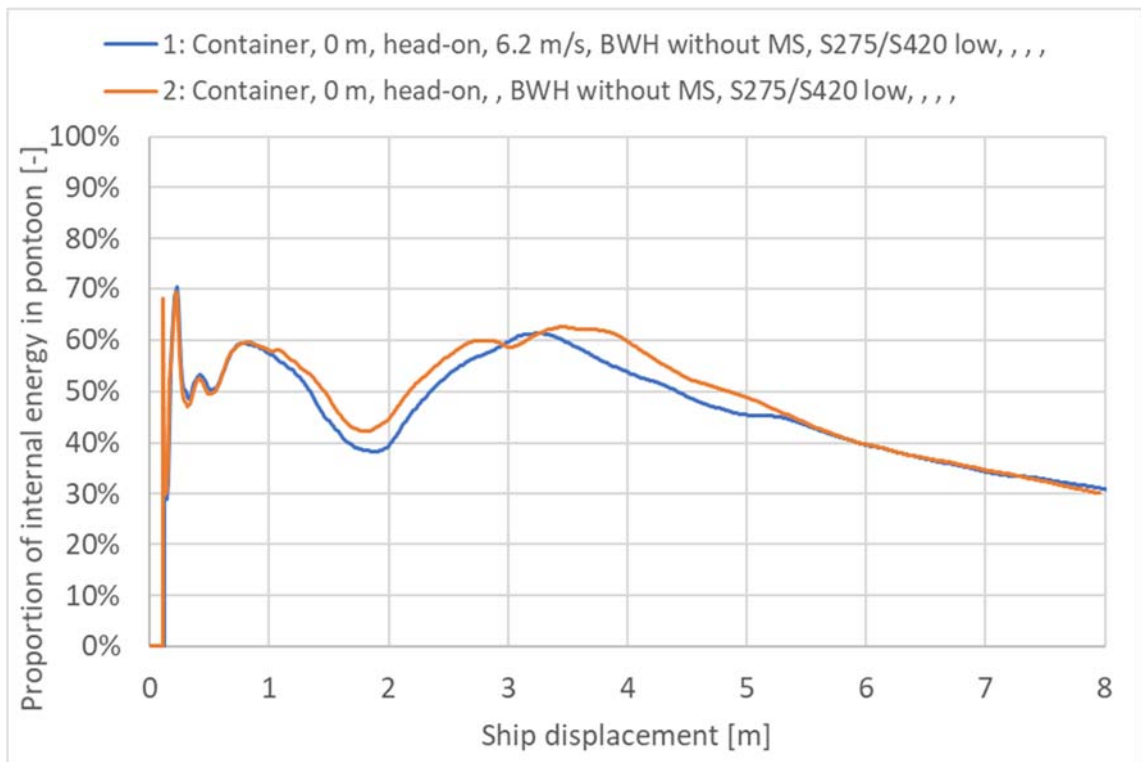


> Figure 6-8 Proportion of internal energy in pontoon [-] impact bow-pontoon, sensitivity of velocity

Figure 6-9 shows a graphical presentation of the sensitivity of impact height and velocity investigated. The maximum force from Figure 6-1 and Figure 6-5 is plotted, defined by a cut-off at ship displacement corresponding 100 MJ for the respective simulation.

The simulation is not very sensitive to the impact velocity. In terms of the maximum contact energy, the simulation is not very sensitive to draught height either. However, as seen in Figure 6-2, the proportion of internal energy in the pontoon and the ship bow changes drastically for the head-on impact with highest energy dissipation in the bow at draught 9.6 m and highest energy dissipation in the pontoon at draught 8.6 m. The latter is used for impact simulations with the container bow.

Figure 6-10 shows the proportion of internal energy in the pontoon for all simulations conducted. Generally, the pontoon dissipates most of the energy while the ship bow is spared. This is conservative when considering damage of the pontoon. There are some exceptions where the ship bow is more damaged. These are head-on impact with draught height 9.6 m of the container bow, the simulations with material damage model FLD or BWH model without mesh scaling and the simulation with full integration of elements.

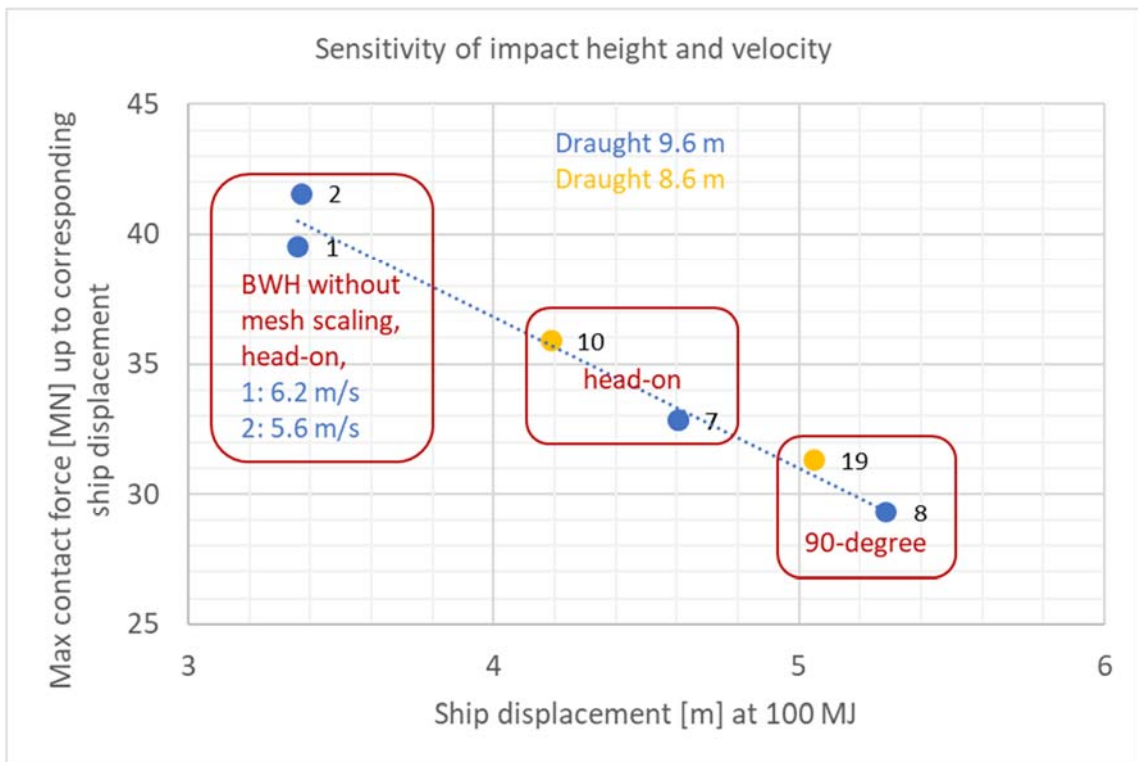


> Figure 6-9 Sensitivity of impact height and velocity

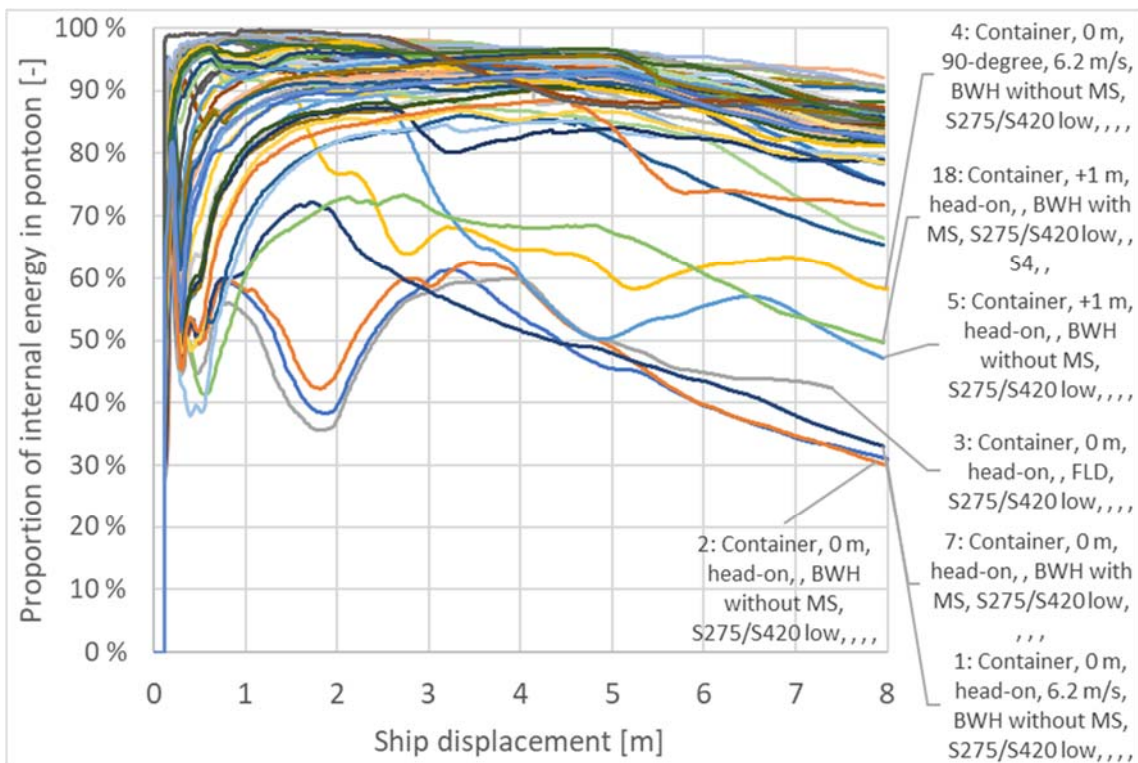


> Figure 6-10 Proportion of internal energy in pontoon [-] impact bow-pontoon, series name of the non-conservative simulations with low proportion of dissipated energy in the pontoon is displayed

7 CONTROL OF ENERGY BALANCE

The energy balance for the simulations in this report is defined as:

$$ETOTAL = ALLKE + ALLIE + ALLFD + ALLVD - ALLWK$$

Total energy = ("Kinetic" + "internal" + "frictional" + "viscous") energy - "external work"

Table 7-1 show the control of energy balance in the last frame (8 m or 16 m ship displacement) for the models in section 5.3.2 [1]. Figure 7-1 to Figure 7-5 show the energy balance graphically.

The error in energy balance of the container bow head-on impact model is a bit higher than the error of the other models displayed. This model has a slightly discontinuous frictional dissipation seen in Figure 5-13 [1]. The discontinuity is due to contact disturbances in the model. The error is small, and the model's behavior is not affected by it. The results are considered credible. Some small disturbances are also seen for a few other models.

Default options to the explicit solver and sections control have been used. Changing the default values may solve the small disturbances observed, but often with the cost of computational time.

> *Table 7-1 Energy balance of the models reported in section 5.3.2 [1]*

	Container, head-on	Container, 90-degree	Ice-strengthened, head-on	Ice-strengthened, 90-degree	Ice-strengthened, 90-degree between bulkheads and frames
ALLKE	235 MJ	234 MJ	235 MJ	235 MJ	240 MJ
ALLIE	224 MJ	184 MJ	135 MJ	120 MJ	265 MJ
ALLFD	40 MJ	40 MJ	48 MJ	38 MJ	159 MJ
ALLVD	5 MJ	2 MJ	2 MJ	1 MJ	1 MJ
ALLWK	260 MJ	224 MJ	184 MJ	159 MJ	430 MJ
ETOTAL	234 MJ	234 MJ	234 MJ	234 MJ	234 MJ
ALLKE + ALLIE + ALLFD + ALLVD - ALLWK	244 MJ	236 MJ	236 MJ	235 MJ	237 MJ
Error	4.1 %	0.9 %	0.6 %	0.5 %	1.2 %
Energy balance ok?	Yes (almost)	Yes	Yes	Yes	Yes

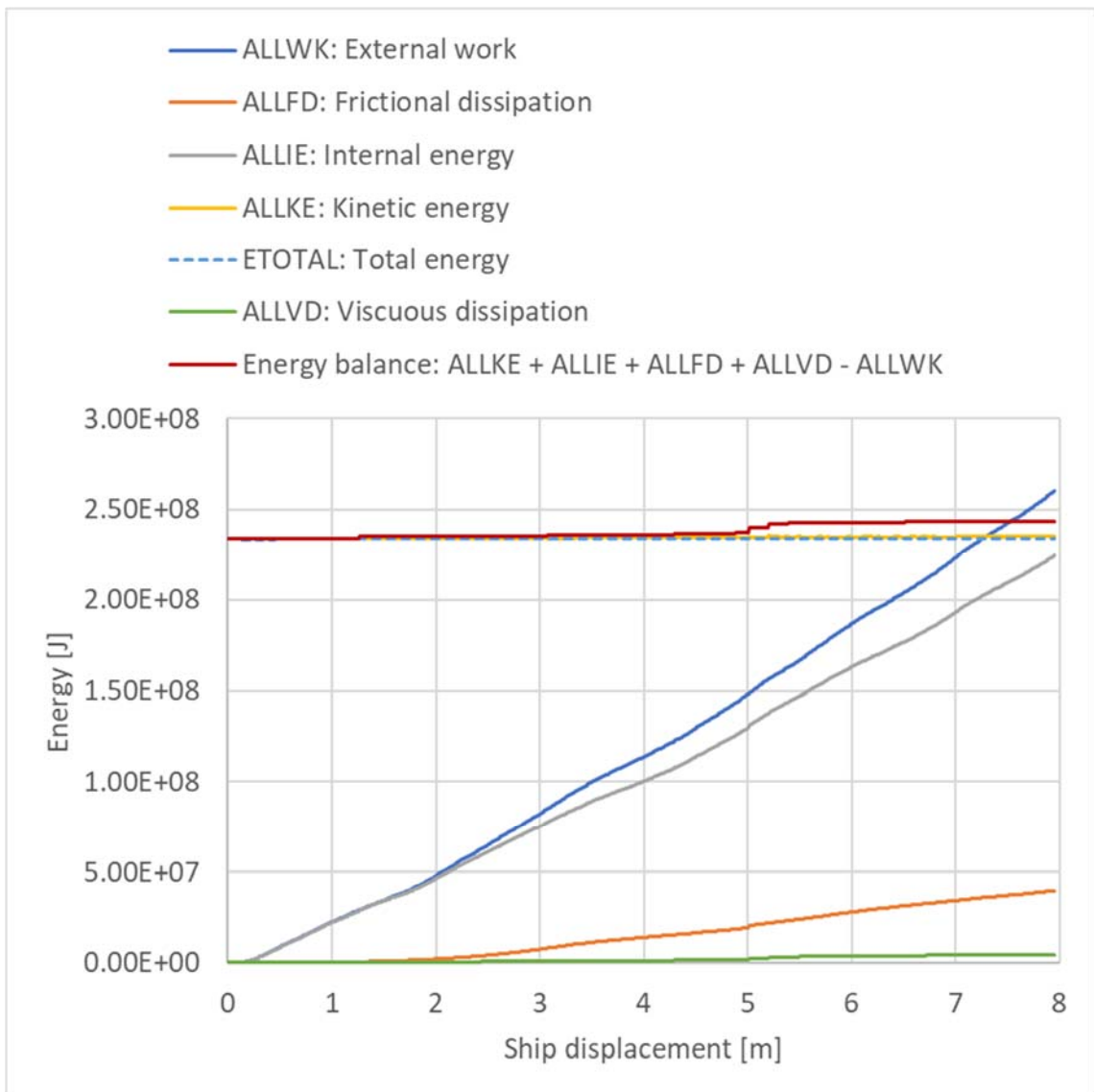


> Figure 7-1 Energy balance of model with ID-no. 55: Base case impact container bow-pontoon head-on

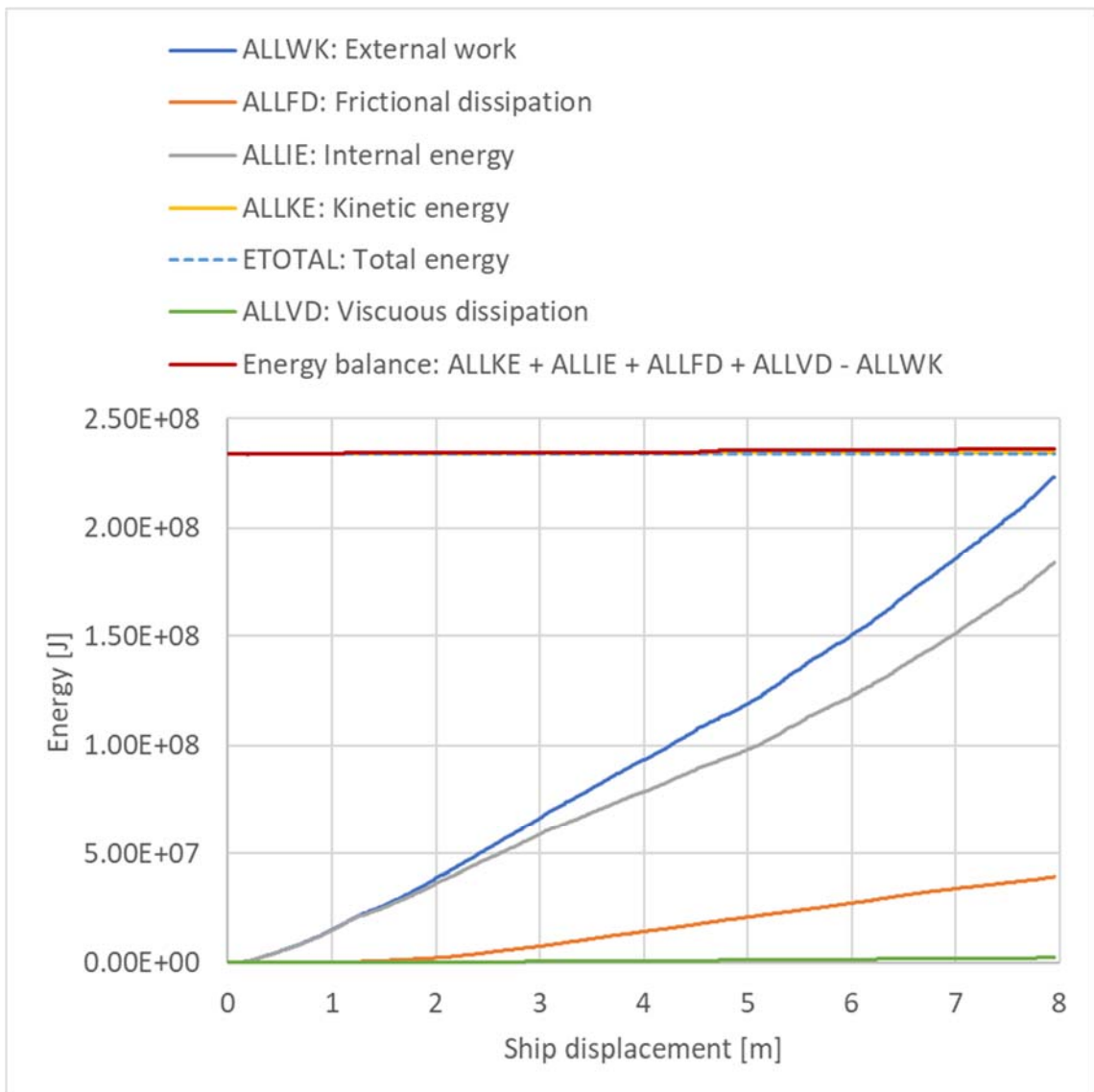


> Figure 7-2 Energy balance of model with ID-no. 52: Base case impact container bow-pontoon 90-degree

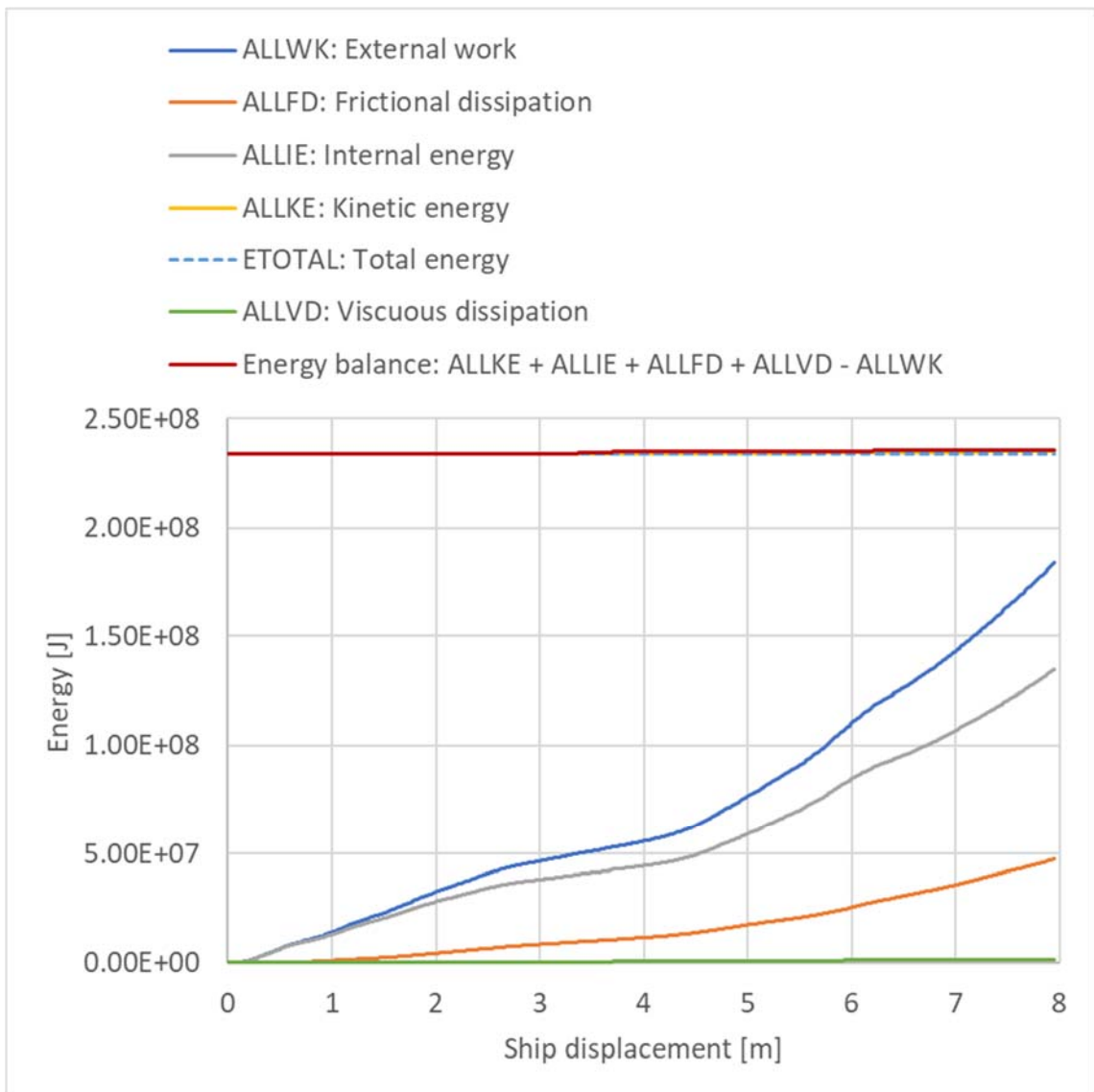


> Figure 7-3 Energy balance of model with ID-no. 48: Base case impact ice-strengthened bow-pontoon head-on

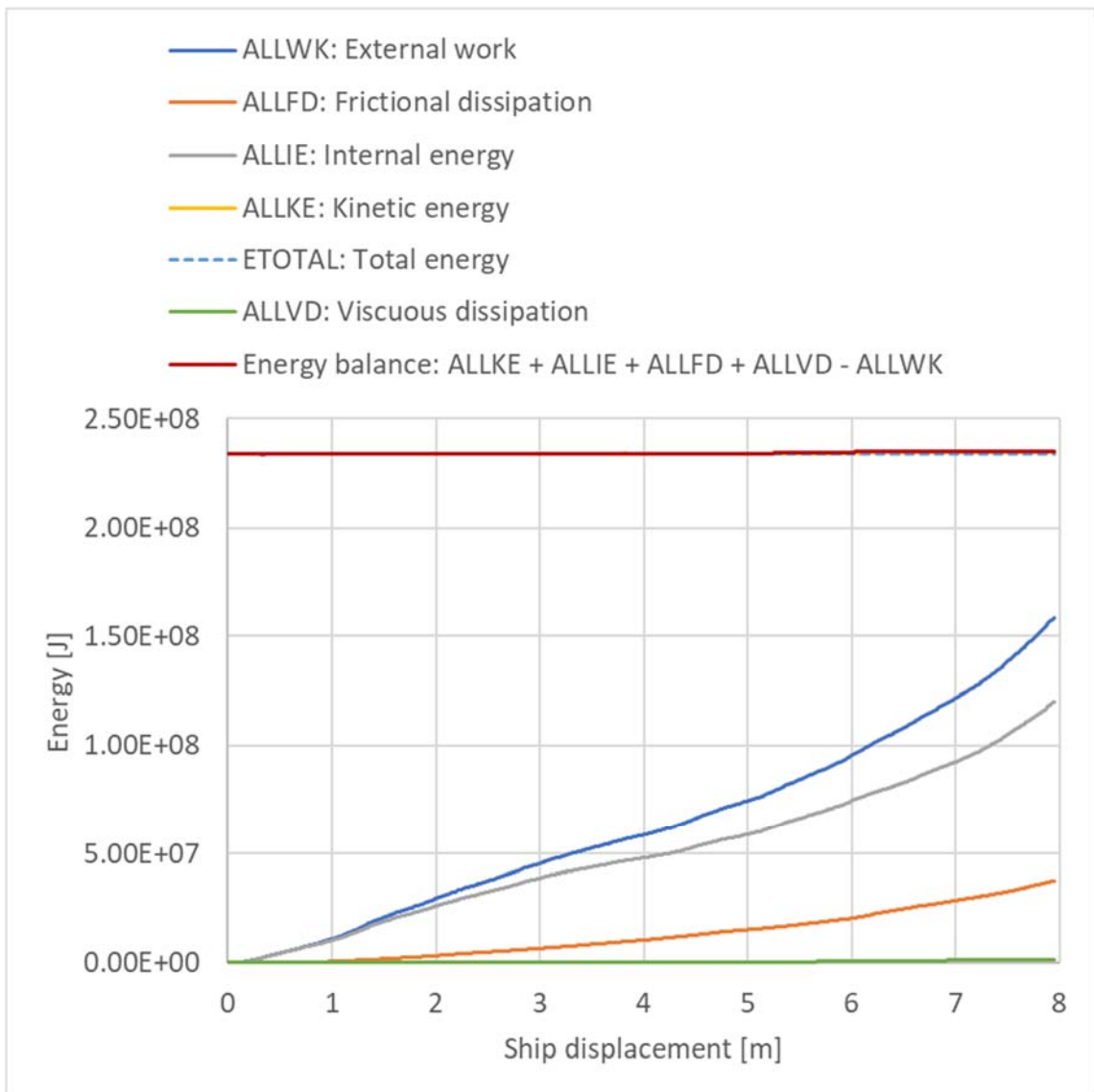


> Figure 7-4 Energy balance of model with ID-no. 49: Base case impact ice-strengthened bow-pontoon 90-degree

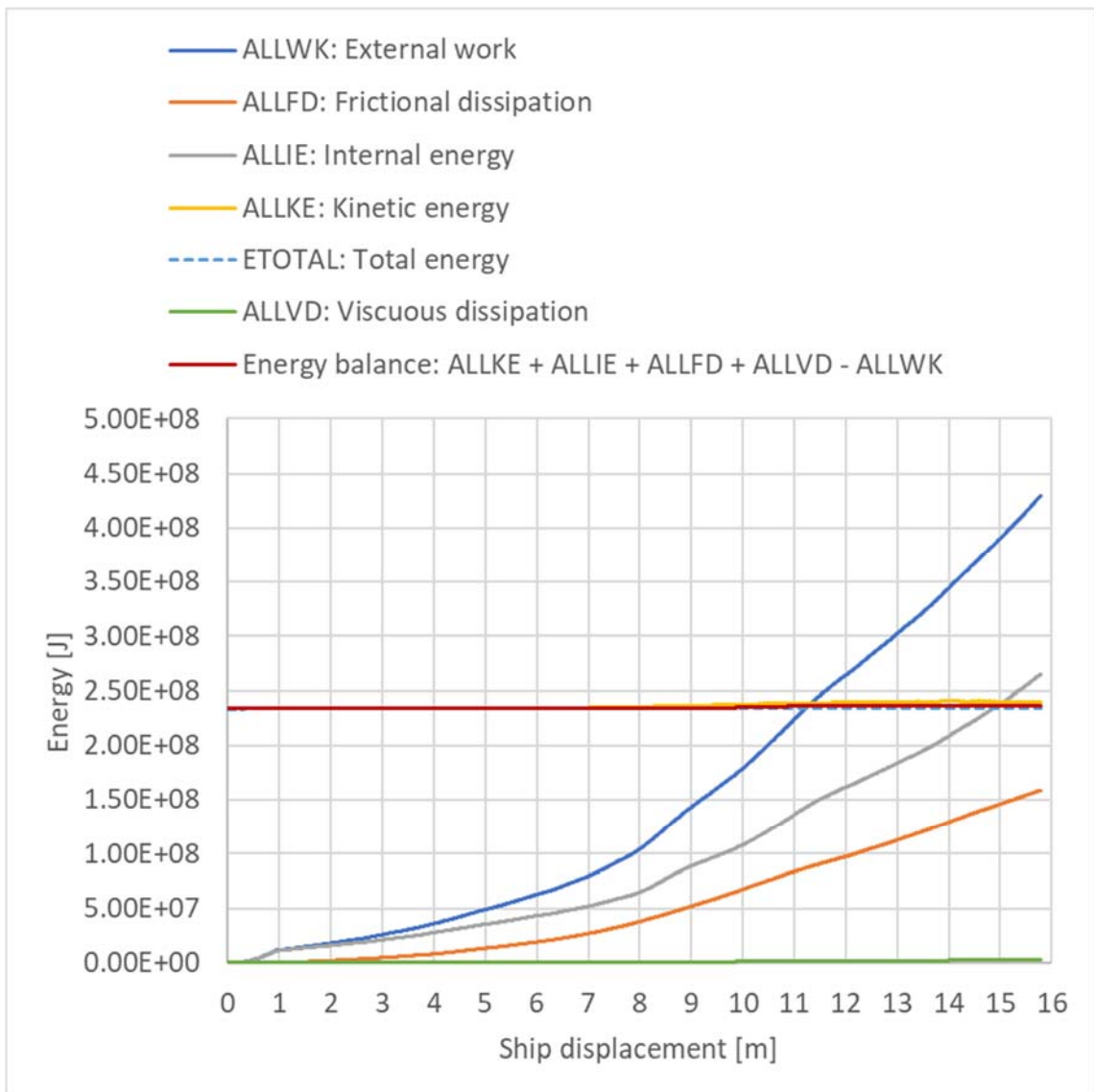


> Figure 7-5 Energy balance of model with ID-no. 63: Base case impact ice-strengthened bow-pontoon 90-degree between bulkheads and frames

8 REFERENCES

- [1] SBJ-33-C5-OON-22-RE-014-B, "Concept development floating bridge E39 Bjørnafjorden - K12 - Ship impact, pontoons and columns," Norconsult, Dr. Techn. Olav Olsen, 2019.
- [2] Y. Sha, I. F. Osvoll and J. Amdahl, "Ship-pontoon collision analysis of the floating bridge concepts for Bjørnafjorden," NTNU, 2018.
- [3] SBJ-20-C3-AAS-27-RE-002, "Bjørnafjorden Suspension Bridge - K1 Impact Report - Local," Aas-Jakobsen, NG,; Johs Holt, Moss Maritime, Plan Arkitekter, Cowi, Aker Solutions, 2017.
- [4] DNVGL-RP-C208, "Determination of structural capacity by non-linear finite element analysis methods," DNV GL, 2016.
- [5] SBJ-33-C5-OON-22-RE-014-B App. B, "K12 - Ship Impact, pontoons and columns, Appendix B - Mesh and material sensitivity study," Norconsult, Dr. Techn. Olav Olsen, 2019.
- [6] SBJ-33-C5-OON-22-RE-013-B, "Concept development floating bridge E39 Bjørnafjorden - K12 - Ship impact, Global assessment," Norconsult, Dr. Techn. Olav Olsen, 2019.
- [7] Simulia, "Abaqus/CAE 2017," Dassault Systèmes, 2016.
- [8] SBJ-32-C4-SVV-90-BA-001, "Design Basis Bjørnafjorden floating bridges," Statens Vegvesen, 2018.